Universitetet i Sørøst-Norge

Masteroppgaven

MPRO5001

Predefinert informasjon

Startdato:	02-04-2019 09:00	**Termin:**	2019 VÅR
Sluttdato:	02-05-2019 14:00	**Vurderingsform:**	Norsk 6-trinns skala (A-F)
Eksamensform:	Masteroppgave		
SIS-kode:	222 MPRO5001 1 MO 2019 VÅR		
Intern sensor:	Trine Langaas		

Deltaker

Navn:	Marina Rønning
Kandidatnr.:	12
USN-id:	883828@usn.no

Marina Rønning

Parapapillary Atrophy

Prevalence and distribution of alpha, beta and gamma parapapillary atrophy identified by the means of spectral domain optical coherence tomography (SD-OCT)
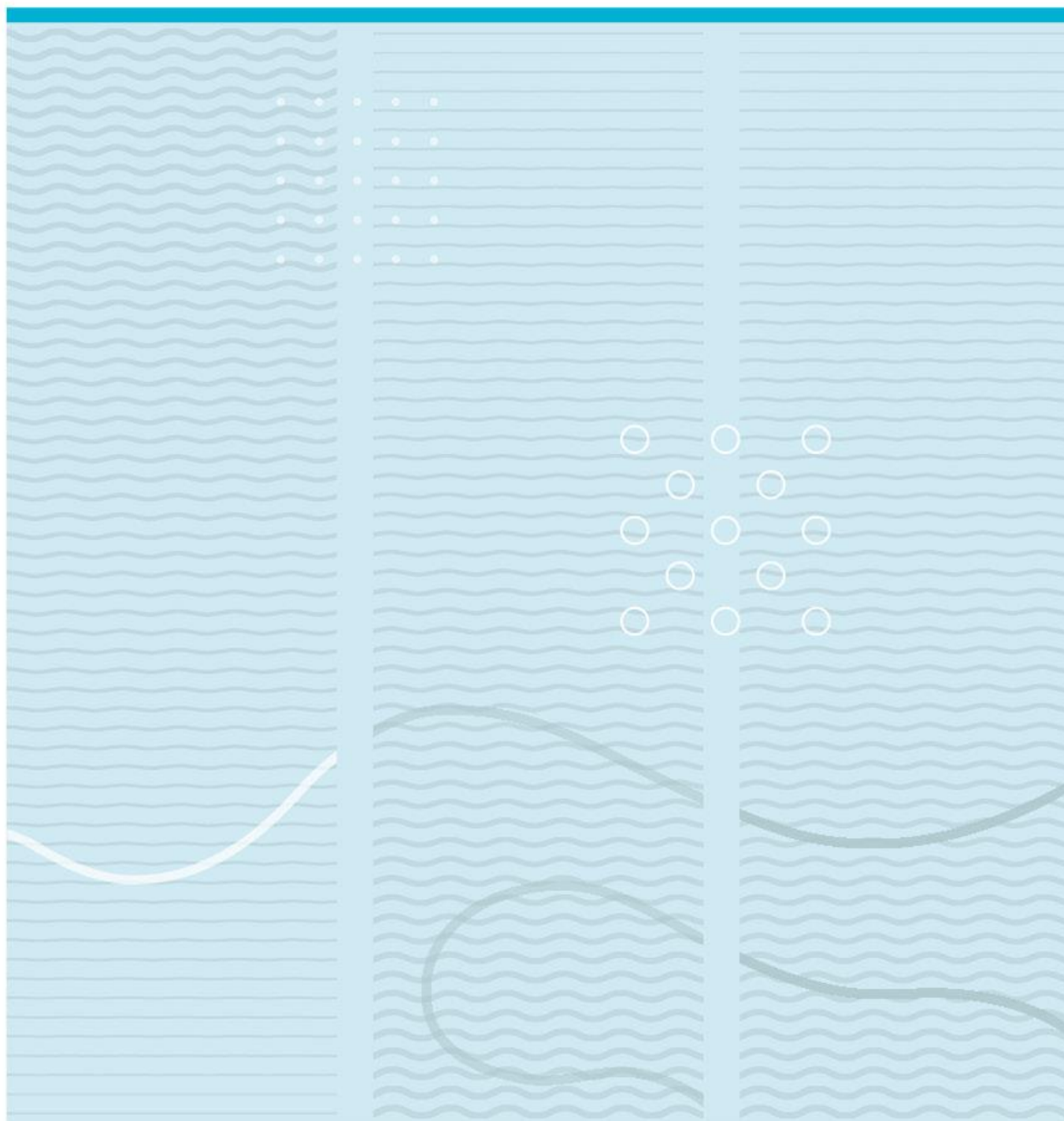
This thesis is worth 30 study points

Summary

Purpose: The purpose of this study was to estimate the prevalence and distribution of alpha, beta and gamma parapapillary atrophy in diabetic adults over the age of 40 years, as identified by the means of spectral domain optical coherence tomography (SD-OCT).

Methods: All subjects underwent anamnesis, subjective binocular refraction and imaging with SD-OCT in both eyes. The obtained OCT sections provided 24 degree sections for assessment of the parapapillary retina, which were analysed for the presence of alpha, beta and gamma parapapillary atrophy.

Results: 135 eyes of 70 subjects, with mean age of 61.33 years (range: 43-81, SD: 9.68) was included. Alpha parapapillary atrophy was found in 100 % of eyes. The atrophy occurred least frequently in the 240 degree section in right eyes, and in the 270 degree section in left eyes, but was evenly distributed in the parapapillary area with frequencies above 90 %. The prevalence of beta parapapillary atrophy was 77.6 % (CI: 67.6, 87.6) in right eyes, 66.2 % (CI: 55.9, 77.4) in left eyes, and was present in both eyes in 60.0 % (CI: 55.9, 77.4) of subjects. The difference in prevalence between right and left eyes was not statistically significant (p = 0.118). The atrophy occurred most often in the 345 degree section in right eyes and in the 15 degree section in left eyes, meaning temporally. Beta parapapillary atrophy was least frequent in the 195 degree section in right eyes and in the 225 degree section in left eyes, in other words nasally and inferonasally, respectively. The distribution of frequencies increased evenly from the least frequent to the most frequent degree section. Gamma parapapillary atrophy was found in 22.4 % (CI: 12.4, 32.4) of right eyes and 22.1 % (CI: 12.2, 32.0) of left eyes, which was not a statistically significant (p = 1.0) difference. Gamma parapapillary atrophy was present in both eyes in 20.0 % (CI: 10.3, 29.7) of subjects. The prevalence was highest in the 345 degree section in right eyes and in left eyes in the 300 degree section, meaning temporally and inferotemporally, respectively. The atrophy was not present in the degree sections from 90 through 225 in right eyes and from 75 through 225 degrees in left eyes. The distribution of frequencies started supratemporal, and had a steady increase towards the temporal and inferior area, before having a smooth decrease towards the inferonasal part.

Conclusion: The findings in this study corroborate with previous studies and provides further clinical knowledge of parapapillary atrophies when using OCT.

Keywords: *SD-OCT, parapapillary atrophy, prevalence, distribution.*

Contents

Foreword

1 Introduction

Parapapillary atrophy is an important part of describing the area surrounding the papilla, and the introduction of new imaging techniques, such as optical coherence tomography (OCT) are contributing to the clinical understanding of this area (Guo et al., 2012; Park et al., 2010).

1.1 Retinal structure in an OCT section

OCT imaging technique visualizes the deeper structures of the retina and is non-invasive while providing a cross-sectional view of the retinal layers (Dai et al., 2013; Lee et al., 2010).

1.1.1 Retinal layers surrounding the papilla

The cross-sectional view provided in an OCT section allows visualization of the retinal layers and landmarks. A study by Staurenghi et al (2014) created a consensus on interpretation of structures identified in an OCT section. The relevant retinal layers for the current study are the nerve fibre layer, ganglion cell layer, inner plexiform layer, inner nuclear layer, outer plexiform layer, outer nuclear layer, external limiting membrane, inner segment-outer segment junction (IS-OS junction), interdigitation zone, and the retinal pigment epithelium and Bruch`s membrane complex (RPE/BM-complex) (Staurenghi et al., 2014). Occasionally, the retinal pigment epithelium and Bruch`s membrane
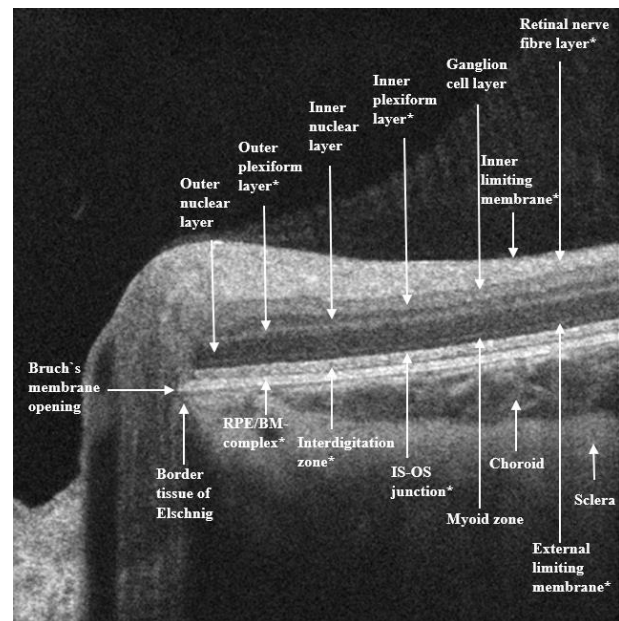
Figure 1-1: *Retinal landmarks in an OCT section.* The retinal layers are seen as hyperreflective (*) and hyporeflective bands in an OCT section, and the choroid and sclera are seen beneath the Bruch`s membrane. The papilla is the "sinkhole" on the left side. RPE/BM = retinal pigment epithelium and Bruch`s membrane. IS-OS = inner segment and outer segment of photoreceptors. Modified from: Staurenghi et al, 2014, p. 1576.

may be two individual layers, where the upper represents the retinal pigment epithelium and the lower represents Bruch`s membrane (Staurenghi et al., 2014). The retinal layers are hyper- and hyporeflective vertical lines in the OCT section, as illustrated in figure 1-1. Beneath the retinal layers, the choroid is visualized as a hypo- and hyperreflective layer, and the sclera might be visible as a hyperreflective area underneath the choroid (Staurenghi et al., 2014).

1.1.2 The border of the papilla in an OCT section

There does not seem to be a consensus on what is regarded as the border of the papilla in an OCT section (Reis et al., 2012). Reis et al (2012) conducted a study to investigate what the ophthalmoscopic border of the papilla, defined as the inner rim of the scleral ring of Elschnig, corresponds to in an OCT section. The findings showed that the ophthalmoscopic border usually corresponded to two structures, or a combination of the two. One of the structures was the border tissue of Elschnig, which is a histologic definition of the previously mentioned ophthalmoscopically defined scleral ring of Elschnig (Reis et al., 2012). This border tissue origins from the anterior edge of the sclera and connects to Bruch`s membrane and is seen as the outermost edge of the choroid in an OCT section, as seen in figure 1-1 (Reis et al., Vianna et al., 2016). The other structure that corresponded to the ophthalmoscopic border was the Bruch`s membrane opening, meaning the ending of Bruch`s membrane (figure 1-1) (Reis et al., 2012).
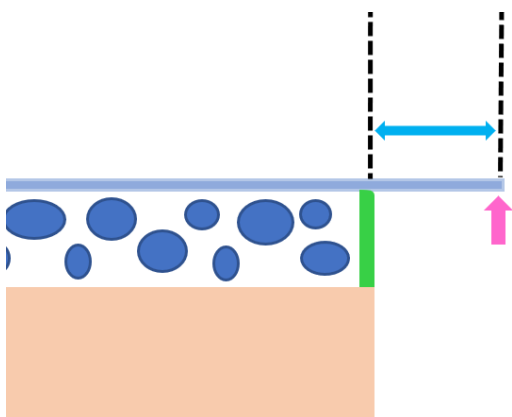
*Figure 1-2: Overhanging Bruch`s membrane.* The figure illustrates Bruch`s membrane (blue line) extending beyond the choroid (white area with blue ovals) and the sclera (orange area) towards the papilla. This overhanging Bruch`s membrane (blue arrow) causes the Bruch`s membrane opening (pink arrow) and the border tissue of Elschnig (green) to have different location. Inspired by Reis et al., 2012, p. 739.

Bruch`s membrane opening and the border tissue of Elschnig might not always be in the same location. In most normal eyes, there has been found an overhanging Bruch`s membrane, both histologically and in OCT sections, meaning that Bruch`s membrane extends beyond the border tissue of Elschnig (figure 1-2) (Curcio et al., 2000; Reis et

al., 2012). This overhanging Bruch`s membrane cannot be differentiated from the scleral ring of Elschnig ophthalmoscopically (Curcio et al., 2000; Reis et al., 2012). Bruch`s membrane might also be misplaced in the other direction, more peripherally than the border tissue of Elschnig, such as in the presence of certain parapapillary atrophies (Dai et al., 2012).

Currently, as mentioned, there is not an agreement in the definition of the border of the papilla in OCT sections. Some studies have used the anterior scleral canal as a definition, since it is proved to be close to the ophthalmoscopic scleral ring of Elschnig, although it is not specified if it's the inner or outer rim of the ring (Miki et al., 2017; Miki et al., 2019). The border tissue of Elschnig is thoroughly investigated, and a recent study by Zhang et al (2018) used the border tissue of Elschnig as their definition of the papilla border (Hayashi et al., 2012; Kim et al., 2013; Vianna et al., 2016). Also, there are studies that have used the inner rim of the scleral ring of Elschnig marked on the infrared ophthalmoscopic image transferred to the OCT section, which is thought to be the same as the border tissue of Elschnig (Dai et al., 2013; Hayashi et al., 2012; Kim et al., 2013; Park et al., 2010; Vianna et al., 2016).

1.2 Classification of parapapillary atrophy

Previously, parapapillary atrophy has been described as either alpha or beta (Hayashi et al., 2010; Jonas et al., 1989; Jonas et al., 2003; Kim et al., 2013; Lee et al., 2010; Miki et al., 2017; Miki et al., 2019). These parapapillary atrophies can be differentiated ophthalmoscopically and has been thoroughly investigated in large population-based studies (Guo et al., 2012; Jonas et al, 1989; Jonas et al., 2003; Ramrattan et al., 1999; Wang et al., 2008). In newer research, however, the classification has been challenged by histologic investigations and the appearance of the atrophies in OCT sections. Consequently, it has been proposed to divide the previous beta parapapillary atrophy into beta and gamma parapapillary atrophy (Dai et al., 2013; Jonas et al., 2012; Jonas et al., 2015; Miki et al., 2017; Miki et al, 2019; Vianna et al., 2016; Zhang et al., 2018).

1.2.1 Alpha parapapillary atrophy

Ophthalmoscopically, alpha parapapillary atrophy is defined as hypo- and hyperpigmentation in the parapapillary area (Guo et al., 2012; Jonas et al., 1989; Jonas et al., 2003; Ramrattan et al., 1999; Wang et al., 2008). The atrophy is adjacent to healthy retina peripherally and either other parapapillary atrophies or the papilla centrally (Guo et al., 2012; Jonas et al., 1989; Jonas et al., 2003; Wang et al., 2008). This definition has been proven to have a significant correlation with the histologic definition; irregularities in the retinal pigment epithelium cells, such as different sizes and different melanin quantity, which causes clumping and irregular arrangement of retinal layers (Curcio et al., 2000; Dichtl et al., 1998; Kubota et al., 1993).

Alpha parapapillary atrophy has not been included in newer studies using OCT, and a clear definition is not provided. Dai et al (2013) and Jonas et al (2015) illustrates the atrophy in OCT sections, using the histologic definition, although no irregularities of the retinal pigment epithelium, as described above, is easily seen in the examples. Lee et al (2010) investigated the area ophthalmoscopically corresponding to alpha parapapillary atrophy in OCT sections, and irregularities of the retinal pigment epithelium was not present in any eyes. They hypothesized that these changes cannot be discovered with current OCTs, because the axial resolution is currently not at a cellular level (Lee et al., 2010).

However, Lee et al (2010) did find a specific finding related to alpha parapapillary atrophy in their study. They observed that the IS-OS junction, representing the transition between the inner and outer segments of the photoreceptors, and the external limiting membrane had gradual thinning when approaching the papilla, described as a tapering loss of tissue (figure 1-3). This gradual thinning was seen in 86.7 percent of the eyes with alpha parapapillary atrophy (Lee et al., 2010). A more abrupt termination of the IS-OS junction was seen when beta parapapillary atrophy was present in the same OCT section (Lee et al., 2010). All retinal layers have been described as present in the alpha area, and as configured in a gentle slope downwards toward the papilla border (Lee et al., 2010).

1.2.2 Beta parapapillary atrophy

Beta parapapillary atrophy is ophthalmoscopically defined as marked atrophy of the retinal pigment epithelium, and the choriocapillaris, with thinning of chorioretinal tissue, which increases the visibility of underlying structures, such as large choroidal vessels and sclera (Guo et al., 2012; Jonas et al., 1989; Jonas et al., 2003; Ramrattan et al., 1999; Wang et al., 2008). Beta parapapillary atrophy is always located more centrally towards the papilla than alpha parapapillary atrophy (Guo et al., 2012; Jonas et al., 1989; Wang et al., 2008). The ophthalmoscopic definition is significantly correlated to histologic appearance of beta parapapillary atrophy (Kubota et al., 1999).

Histologically, the atrophy is defined as an area with complete loss of retinal pigment epithelium with an intact Bruch`s membrane, which might be thickened, an incomplete loss of photoreceptors and a closure of choriocapillaris (Curcio et al., 2000; Jonas et al, 2011; Jonas et al, 2012; Kubota et al., 1993).

In OCT sections, beta parapapillary atrophy is defined as an area devoid of retinal pigment epithelium but with an intact Bruch`s membrane, which might be thickened, as seen in figure 1-3 (Dai et al., 2013; Hayashi et al., 2012; Jonas et al., 2015; Kim et al., 2013; Lee et al., 2010; Miki et al., 2017; Miki et al., 2019; Vianna et al., 2016; Zhang et al., 2018). Therefore, beta parapapillary

Figure 1-3: Parapapillary atrophies in an OCT section. The figure shows a schematic drawing of the parapapillary atrophies linked to an OCT section. Alpha (α) is seen between the gradually terminating IS-OS junction (green line) and the termination of the retinal pigment epithelium (light blue line). Beta (β) is seen between the ending of the retinal pigment epithelium and the ending of Bruch`s membrane (dark blue line). Gamma (γ) is seen as bare sclera (orange area). The line to the far left represents the border tissue of Elschnig.

atrophy is regarded as the area between the ending of retinal pigment epithelium and the ending of Bruch`s membrane (Dai et al., 2013; Hayashi et al., 2012; Kim et al., 2013; Lee et al., 2010; Miki et al., 2017; Miki et al., 2019; Vianna et al., 2016; Zhang et al., 2018). The lack of retinal pigment epithelium causes hyper reflectance of the choroid, which has been found in 100 percent of eyes within the area of ophthalmoscopically

identified beta parapapillary atrophy in OCT sections (Hayashi et al., 2012; Lee et al., 2010). Other retinal layers, from the ganglion cell layer to and including the outer nuclear layer, have been described as tapering fragments, or lacking over the atrophy, and as mentioned, the IS-OS junction ends peripheral to the distal border of the atrophy (Hayashi et al., 2012; Lee et al., 2010).

1.2.3 Gamma parapapillary atrophy

Gamma parapapillary atrophy has the same ophthalmoscopic appearance as beta parapapillary atrophy, and cannot be differentiated ophthalmoscopically (Dai et al., 2013; Jonas et al., 2015). Histologically, gamma parapapillary atrophy corresponds to a marked elongated and thinned sclera with overlying retinal nerve fibre layer, devoid of Bruch`s membrane, choroid, retinal pigment epithelium and deeper retinal layers, and was described as early as 1998 (Dichtl et al., 1998; Jonas et al., 2011; Jonas et al., 2012). In easier terms, it is the same as beta parapapillary atrophy, but without Bruch`s membrane, deeper retinal layers and choroid.

The definition of gamma parapapillary atrophy seen in an OCT section is identical to the histological definition, meaning sclera without Bruch`s membrane and choroid (Dai et al., 2013; Jonas et al, 2015; Miki et al., 2017; Miki et al., 2019; Vianna et al., 2016; Zhang et al., 2018). It is regarded as the area between the ending of an intact Bruch`s membrane and the border of the papilla, as seen in figure 1-3 (Dai et al., 2013; Jonas et al., 2015; Zhang et al., 2018). The atrophy is always adjacent to the border of the papilla, and therefore, more central than alpha and beta parapapillary atrophy (Dai et al., 2013; Jonas et al., 2015; Zhang et al., 2018).

1.3 Prevalence and distribution of parapapillary atrophy

The knowledge regarding prevalence and distribution of parapapillary atrophy is greater ophthalmoscopically than in OCT sections. Alpha parapapillary atrophy has not been included in most OCT research, and the studies using OCT when investigating beta and gamma parapapillary atrophy has mostly been focused on areal, rather than the prevalence and distribution.

1.3.1 Prevalence and distribution of alpha parapapillary atrophy

Ophthalmoscopically, prevalence of alpha parapapillary atrophy has been found to vary between 54.0 and 98.6 percent in normal eyes (Jonas et al, 1989; Jonas et al., 2003; Ramrattan et al., 1999; Wang et al., 2008). The difference in prevalence in the different studies might be explained by variations in the study population. Alpha has been found to be occur significantly more often than beta parapapillary atrophy (Jonas et al., 1989; Jonas et al., 2003). It occurs most often in the temporal parapapillary area, followed by the inferior, superior and nasal area, in that order (Jonas et al, 1989; Jonas et al., 2003; Wang et al., 2008). Lee et al (2010) conducted the only study using OCT, or more specifically spectral domain (SD)-OCT, that includes alpha parapapillary atrophy, and the prevalence was 100 percent in the temporal parapapillary area of all eyes.

1.3.2 Prevalence and distribution of beta parapapillary atrophy

The prevalence of ophthalmoscopically defined beta parapapillary atrophy has been found to vary between 11.4 and 19.9 percent in normal eyes (Jonas et al, 1989; Jonas et al., 2003; Ramrattan et al., 1999; Wang et al., 2008). The differences might be explained by the same factors that for alpha parapapillary atrophy. Equally to alpha, beta parapapillary atrophy has been found most often temporally, followed by inferiorly, superiorly and nasally, in that order (Jonas et al, 1989; Jonas et al., 2003; Wang et al., 2008). Using SD-OCT, Lee et al (2010) found the prevalence of beta parapapillary atrophy to be 75.0 percent of eyes. Hayashi et al (2012) reported a prevalence of 63.0 percent when investigating with SD-OCT. New research from Zhang et al (2018) using SD-OCT detected beta parapapillary atrophy in 72.6 percent of eyes. They also investigated the distribution and concluded that it was most often found temporally and rarely found nasally (Zhang et al., 2018).

1.3.3 Prevalence and distribution of gamma parapapillary atrophy

Most studies using OCT when investigating prevalence were executed before the classification of beta parapapillary atrophy was divided into beta and gamma. Lee et al (2010) described a step configuration of the parapapillary scleral bed, which Dai et al (2013) and Jonas et al (2012) has interpreted as gamma parapapillary atrophy, and it occurred in 5.0 percent of normal eyes. They also discovered that it was only seen in the

inferotemporal half of the parapapillary area (Lee et al., 2010). Hayashi et al (2012) reported finding beta parapapillary atrophy, using SD-OCT, with a defect Bruch`s membrane in 28.0 percent of normal eyes, which Dai et al (2013) and Jonas et al (2012) later has interpreted as gamma parapapillary atrophy. New research using SD-OCT found gamma parapapillary atrophy to be present in 26.3 percent of normal eyes (Zhang et al., 2018). Like beta parapapillary atrophy, it occurred most often temporally, and rarely nasally (Zhang et al., 2018).

1.4 Importance of evaluating parapapillary atrophy

Although the pathophysiology of parapapillary atrophies is unknown, there has been many studies regarding the clinical significance of parapapillary atrophy (Park et al., 2010; Ramrattan et al; 1999). The presence of alpha parapapillary atrophy is associated with age and glaucoma, but the diagnostic value is limited, since the prevalence is high in normal populations (Jonas et al., 1989; Ramrattan et al., 1999; Wang et al., 2008). Presence of beta parapapillary atrophy also has a significant association with glaucoma and age, and to a lesser extent myopia (Hayashi et al., 2012; Jonas et al, 1989; Kim et al., 2013; Wang et al 2008; Zhang et al, 2018). Presence of gamma parapapillary atrophy, on the other hand, has been found to be significantly associated with myopia and longer axial length and is most likely caused by elongation of the globe (Hayashi et al., 2012; Kim et al., 2013; Zhang et al., 2018). As for association with each other, the presence of alpha parapapillary atrophy and beta has been found to be significantly connected, and beta is seldom present without alpha (Jonas et al., 2003). Gamma and beta parapapillary atrophy, on the other hand, has not been found to be significantly associated, suggesting that they do not occur directly dependent of each other (Dai et al., 2013; Jonas et al, 2015; Vianna et al., 2016).

2 Purpose of study

The main purpose of this study was to estimate the prevalence and distribution of alpha, beta and gamma parapapillary atrophy in diabetic adults over the age of 40 years, as identified by the means of SD-OCT.

2.1 Research questions

The purpose of the study was based on these research questions:

- In a sample of diabetic adults over the age of 40 years, what is the frequency of alpha parapapillary atrophy identified with SD-OCT in one and both eyes?
- When alpha parapapillary atrophy is present in an eye, where is the atrophy most commonly present and how is it distributed in the parapapillary area?
- In a sample of diabetic adults over the age of 40 years, what is the frequency of beta parapapillary atrophy identified with SD-OCT in one and both eyes?
- When beta parapapillary atrophy is present in an eye, where is the atrophy most commonly present and how is it distributed in the parapapillary area?
- In a sample of diabetic adults over the age of 40 years, what is the frequency of gamma parapapillary atrophy identified with SD-OCT in one and both eyes?
- When gamma parapapillary atrophy is present in an eye, where is the atrophy most commonly present and how is it distributed in the parapapillary area?

2.2 Significance of study

Clinical differentiation between beta and gamma parapapillary atrophy is advantageous and can be easily achieved by the means of OCT in clinical practice, given adequate knowledge for interpretation (Dai et al., 2013; Miki et al., 2017; Miki et al., 2019; Vianna et al., 2016). Additionally, there is lack, or limitations, of research regarding the prevalence and distribution of alpha, beta and gamma parapapillary atrophy. To my knowledge, there are currently no studies that have investigated the prevalence and distribution of all three atrophies in one study. The current study is expected to provide

knowledge for optometrists which can be used in clinical practice for interpretation of parapapillary atrophy in OCT sections.

3 Methods

The current study has been executed in collaboration with a larger research study, "Diabetes, Vision and Eye Health" (DVOH-project), where three supervisors (P.O.L., T.L.M., V.S.) and five master students (H.K.F., J.A., J.L.P., M.R., S.S.) participated at the time of collaboration. Further methodology will mainly describe the methods for the presented study.

3.1 Study design

The study was in cross-sectional study design.

3.2 Study sample

3.2.1 Target population

The target population was adults over the age of 40 years in Norway.

3.2.2 Study population

The population eligible to participate in the study were males and females, over the age of 40 years, who participated in the DVOH-project in the period of 1st of August 2018 till 28th of January 2019. Because of the collaboration with the DVOH-project, type II diabetes mellitus was a criterion for participation. There has not been found an association with diabetes mellitus and parapapillary atrophy (Guo et al., 2012; Kim et al., 2013; Zhang et al., 2018).

3.2.3 Exclusion criteria

Exclusion criteria was based on the placement of the scan pattern of the OCT and the quality of the OCT sections;
- Missing image: exclusion of the relevant eye.

- Misalignment of scan pattern outside of the papilla border, causing a misplacement of all OCT sections compared to the intendent location: exclusion of the relevant eye (further explanation provided in section 3.5.2).
- Misalignment of scan pattern outside the central 20 percent of the papilla, causing a misplacement of most OCT sections compared to the intendent location: exclusion of all OCT sections except the one in the direction of the misalignment, and one section immediately adjacent to each side (further explanation provided in section 3.5.2).
- Inadequate image quality causing uncertain visualization of the retinal layers and the distal border of the relevant parapapillary atrophy (e.g. shadows from blood vessels or floaters, blur): exclusion of the specific degree section for the specific parapapillary atrophy.

3.3 Recruitment

Recruitment of participants were a collaboration between supervisors and master students in the DVOH-project. The supervisors (T.L.M., V.S.) gave lectures to local diabetes-gatherings and invited them to participate. They also hung up notes at doctors' offices with brief information and contact information, as well as in an ophthalmologist's office. In addition, they featured in a local newspaper, an optometrist magazine and a national newspaper, where the DVOH-project was mentioned. The master student's (H.K.F., J.L.P., S.S., M.R.) responsibility was to call optical stores in the three nearest counties (Buskerud, Telemark and Vestfold), to provide them with information and ask for participation in recruiting subjects for the research project. The stores that wanted to recruit, received necessary contact information and a poster from the supervisors. The recruitment for the presented study was continuous throughout the fall of 2018, starting from 1st of August.

The subjects that wanted to participate, contacted the supervisors and submitted their contact information. For booking of appointments, the possible subjects were called by either another master student (H.K.F.) or the main observer (M.R.). In these conversations, information about the examination was repeated, and the possible subjects were encouraged to ask questions. The subjects that wanted to participate was given an appointment and received an e-mail with the consent form (Annex 1). The

subjects and the respective examining master student signed two copies of the consent form at the time of the examination. A subject was considered included in the study when the consent form was signed of both parties. For this specific project, the recruitment and booking ended 3rd of December 2018, with examinations booked until 28th of January 2019. Included subjects are therefore those who had signed the consent form within the time frame from 1st of August 2018 till 28th of January 2019.

3.4 Protocol

The relevant procedures for this study, which includes demographic information and OCT-imaging, were a part of an examination which included many procedures for the DVOH-project. The duration of the examination was approximately three hours, and included standard initial testing, standard subjective refraction, evaluation of anterior segment and dry eye, and evaluation of posterior segment with different imaging modalities and perimetry. The relevant procedures for the presented study were estimated to last about 40 minutes, including 20 minutes for response time of eye drops. Tropicamide minims 0,5 percent were used on all subjects for dilating the pupil. Both eyes of a subject were examined. The examinations were performed by the five master students, including the main observer.

3.4.1 Demographic information

Demographic data was obtained through anamnesis and refraction. The refraction was executed with the standardized method of subjective binocular refraction. The registration of this data was done by each master student on a manual registration form for the DVOH-project, which was kept in a locked cabinet with limited access, with each subject having their own folder with individual journal numbers.

3.4.2 Imaging with SD-OCT

3.4.2.1 Specifications of SD-OCT and scan pattern

Cirrus HD-OCT (model 5000, software version 8.0, Carl Zeiss Meditec, Inc., Dublin, CA) was used to obtain the images. The instrument uses a super luminescent diode,

with a wavelength of 840 nanometers, to acquire the OCT sections. The scan speed is 27 000 A-scan per second, with axial resolution of five microns and transverse resolution of 15 microns in tissue (Carl Zeiss Meditec, 2014). HD Radial scan pattern was used for imaging, which includes 12 high definition radial scan lines with a scan depth of two millimeter. Each line is composed of 8 B-scans that contain 1024 A-scans.
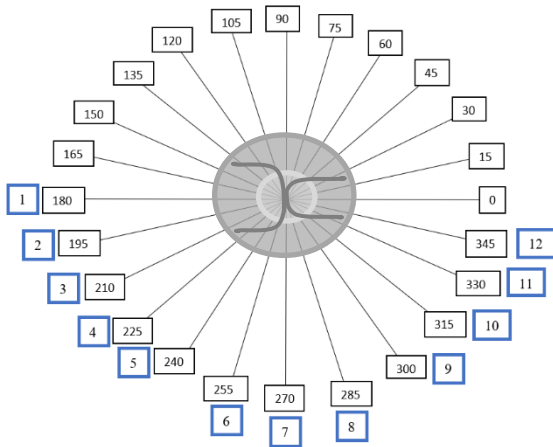
Figure 3-1: HD Radial scan pattern. The figure illustrates the scan lines (blue) in the scan pattern, around a schematic papilla, and shows the OCT sections with degree sections that is represented in each scan line. The identification of the scan lines is the same for both eyes, meaning 0 is nasal in right eyes and temporal in left eyes.

The resolution of resulting OCT sections is 938 x 625. OCT section refers to the cross-sectional image resulting from each scan line. The 12 scan lines are labeled with identification numbers from 1 through 12 in the software (figure 3-1). Number 1 represents the OCT section containing the degree sections of 180 and 0 degrees, continuing till 12 in 15-degree intervals in a counter-clockwise direction. Degree sections refer to the degrees represented on each side of the papilla in an OCT section. The identification of scan lines in the software is equal for both eyes, meaning 0 is nasal in right eyes and temporal in left eyes. The radial scan provides a 360-degree cross-sectional view, in sectional 15-degrees, and has been used in previous studies for investigation of the respective area (Lee et al., 2010; Vianna et al., 2016; Zhang et al., 2018).

3.4.2.2 Procedure

All observers had the appropriate standardized protocol available (Annex 2), and the main observer took some random samples of the OCT sections in the beginning of the examination period, to ensure that the procedure was followed. For imaging of the papilla and adjacent area, the fixation target was placed one step nasally, for centration over the papilla. If the scan pattern was not centrally placed over the papilla, the protocol instructed the operator to relocate it to the presumed geometrical center by dragging the pattern on the screen. The length of the scan lines was set to the default

setting of six millimeters, since it gives a satisfying coverage of the parapapillary area. The imaging was executed on both eyes, right first, in dimmed room illumination. Since the imaging was performed by several observers, the quality indicators on the instrument was used for indication of adequate or inadequate quality. The level for acceptance was equal to or above six, and if failed, imaging process should be repeated till wanted quality indication was achieved. If this was not possible for any reason, such as cataract or poor fixation, the observer had to decide when to terminate the procedure. Since the quality was rechecked by the main observer when analyzing the OCT sections, the lack of fulfillment of the quality indicators was not an exclusion criterion.

3.4.3 Data management

The infrared images and the OCT sections were saved as anonymous tiff-files without inherent personal information on a password protected, crypted flash drive. The file names were a combination of identification number, identification of eye, and the two degree sections represented in the OCT section, or alternatively marked as infrared image. The identification number was linked to the journal number of the individual through a code key, which was saved in a research repository (Figshare: https://figshare .com/) with limited access. The identification number was a random number between 1 and 70, and right or left eye was marked with RE or LE. The files names were therefore in the format of ID_EYE_degree section_degree section (e.g. 15_LE_210_30). The highest value for the degree sections represented in the OCT section were always first, to ensure that the files were automatically stored in the correct order for analyses. If more than one set of OCT sections were available, the set of sections with the least misalignment of the scan pattern, or best quality, was chosen. The quality of the infrared image was not relevant.

3.5 Analyses of images

3.5.1 Specifications for analyses

All images were assessed on an Acer LCD-screen with a resolution of 1680 x 1050, and pixel per inch of 90, by the main observer (M.R.). The contrast and luminance of the screen were 100 percent. Evaluations were executed in dimmed room lighting, with

illuminance between 200 and 250 lux. The evaluation began at subject number 1, right eye first, and continued till 70 in the same manner. All infrared images and OCT sections were evaluated with 100 percent magnification in the image processing program ImageJ (National Institutes of Health, version 1.52k, 2019). All images were evaluated twice, the second time after all images had been evaluated once. The second evaluation was used in the study.

3.5.2 Assessment of scan centration in the papilla

The circle tool was used to draw an oval on the presumed distal rim of the visible papilla on the infrared image, which made it approximately the same size as the papilla. The size of the oval, in the form of height and width, was given in pixels. If the infrared image was of inadequate quality, meaning the border of the papilla could not be seen, the OCT sections was used to estimate the location of the border on the infrared image. If the scan pattern was misaligned outside the oval, the whole eye would be excluded from the study. If the scan pattern was inside the border, a smaller oval was drawn, corresponding to 20 percent of the original larger oval. This was done by multiplying the height and width, in pixels, of the larger oval by 0.2 and drawing the smaller oval with the calculated values. The smaller oval was then placed in the presumed center of the visible papilla (figure 3-2). If the center was misaligned outside the small oval, all OCT sections except the one in the direction of the misalignment and one immediately adjacent to each side was excluded. The direction of misalignment was defined as the direction of the middle scan line in the small oval, when it was centered in the papilla.
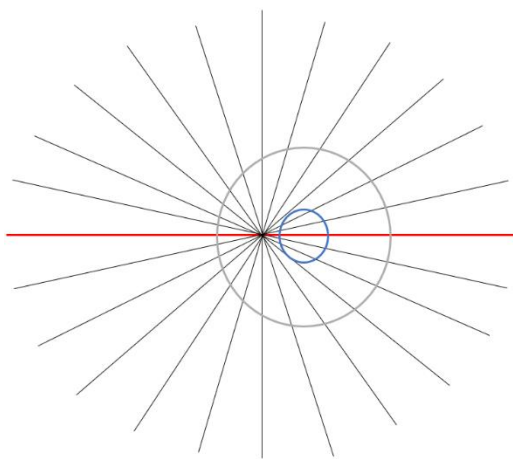

Figure 3-2: Misalignment of scan pattern. Illustration of misalignment of the scan pattern outside of the central 20 percent (blue circle) of the papilla (grey circle), in the direction of 180 and 0 degrees (red line) (e.g. exclusion of all, except 180/0, 195/15 and 210/30).

3.5.3 Evaluation of parapapillary retina

The analysis of the parapapillary area started in the first included OCT section from and including the 0 and 180 degree sections, and in a counter-clockwise direction. Presence of alpha parapapillary atrophy in both degree sections in the OCT section was assessed first, followed by beta and gamma, respectively. The visibility of relevant retinal layers and the distal border of each atrophy was evaluated, and the respective degree section was included or excluded subsequently. All findings were registered on a manual registration form (Annex 3). The analyses of the parapapillary area continued with all included OCT sections in a counter-clockwise direction.

3.5.3.1 Alpha parapapillary atrophy

For the purpose of this study, alpha parapapillary atrophy was defined as a gradual or abrupt ending of the IS-OS junction, seen as the third lowermost hyperreflective layer in OCT sections. A gradual ending was defined as a tapering loss of density to the extent that the IS-OS junction could not be differentiated from the interdigitation zone, seen as the second lowermost hyperreflective layer, and the exact point of termination of the IS-OS junction could not be certainly determined. An abrupt ending was defined as sudden termination of the IS-OS junction, without confusion with the interdigitation zone and with a definite point of termination, as seen in figure 3-3 (Lee et al., 2010). If there was

Figure 3-3: Alpha parapapillary atrophy. The illustration shows gradual ending of IS-OS-junction in the upper degree section, and abrupt ending in the middle degree section. Alpha parapapillary atrophy is the area between the definitively seen IS-OS junction (green arrowhead) and the border tissue of Elschnig (white arrowhead), or the ending of retinal pigment epithelium with presence of beta parapapillary atrophy in the same degree section (blue arrowhead). No parapapillary atrophy is present in the lowermost degree section.
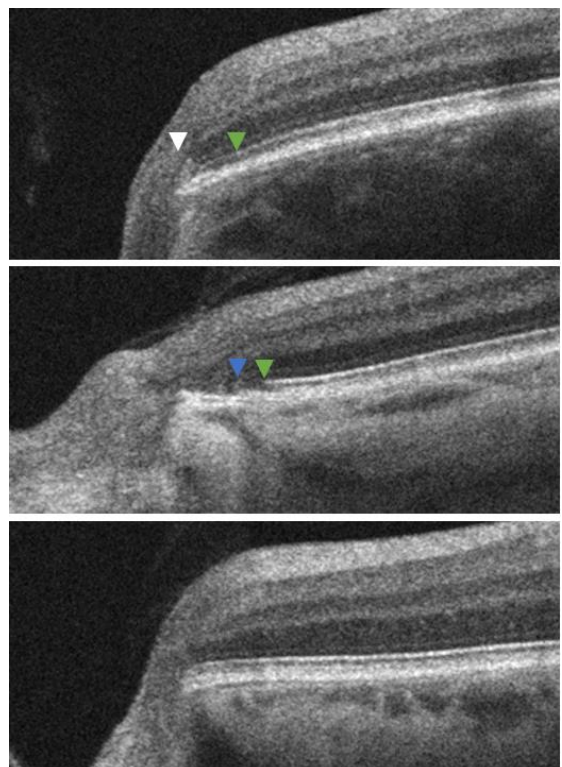
a gradual ending, the IS-OS junction could reach the edge of the optic disc, defined as the border tissue of Elschnig, seen as the border between hypo- and hyperreflective choroid and the darker neural tissue (Reis et al., 2012). There were no alpha parapapillary atrophy present if the IS-OS junction reached the border tissue of Elschnig without a tapering loss of tissue (figure 3-3). Therefore, alpha parapapillary atrophy was regarded as the area between the definitively intact IS-OS junction and the border tissue of Elschnig, alternatively the ending of retinal pigment epithelium in presence with other parapapillary atrophies, as shown in figure 3-3. Alpha parapapillary atrophy was registered as present with gradual ending of IS-OS junction, present with abrupt ending of IS-OS junction, absent, or uncertainty of presence, in all included degree sections and in total for right eye, left eye and both eyes. Uncertainty was defined as uncertain differentiation between the IS-OS junction and other retinal layers, or indistinguishable distal border, caused by other reasons than the exclusion criteria.

3.5.3.2 Beta parapapillary atrophy

For this study, beta parapapillary atrophy was defined as an area devoid of retinal pigment epithelium, seen as the upper part of the lowermost hyperreflective RPE/BM-complex, but with intact Bruch`s membrane, seen as the lower part of the lowermost hyperreflective RPE/BM-complex or as a single hyperreflective lowermost layer (when denuded of retinal pigment epithelium), as seen in figure 3-4 (Dai et al., 2013; Hayashi et al., 2012; Kim et al., 2013; Lee et al., 2010; Miki et al., 2017; Miki et al., 2019; Vianna et al., 2016; Zhang et al., 2018). Bruch`s membrane could be interpreted as thickened in the area, and there could be hyper reflectance of the choroid (Hayashi et al., 2012; Lee et al., 2010). Beta parapapillary atrophy was regarded as the
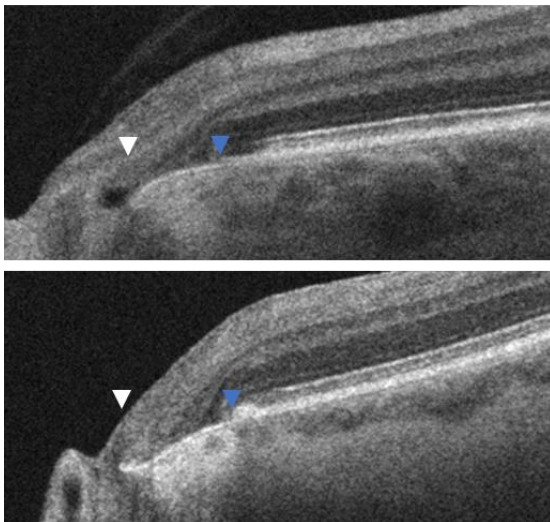

Figure 3-4: Beta parapapillary atrophy. The degree sections show presence of beta parapapillary atrophy between the ending of the retinal pigment epithelium (blue arrowhead) and border tissue of Elschnig (white arrowhead).

area from the ending of intact retinal pigment epithelium to border tissue of Elschnig, as

defined previously, or the ending of Bruch`s membrane in presence with gamma parapapillary atrophy.

As described initially, an overhanging Bruch`s membrane may look similar to beta parapapillary atrophy, and therefore, this was also evaluated in the current study. The presence of overhanging Bruch`s membrane was only assessed in OCT sections without beta parapapillary atrophy. Overhanging Bruch`s membrane was defined as a denuded Bruch`s membrane that extended beyond the border tissue of Elschnig, as defined previously (figure 3-5) (Reis et al., 2012).
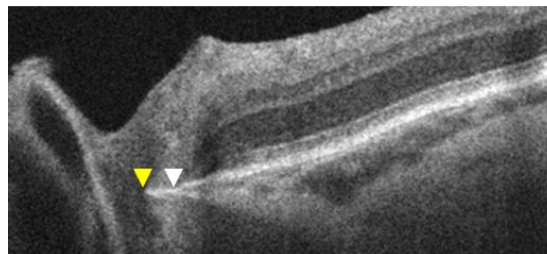
*Figure 3-5: Overhanging Bruch`s membrane.* The degree section illustrates overhanging Bruch`s membrane between the border tissue of Elschnig (white arrowhead) and the Bruch`s membrane opening (yellow arrowhead).

Presence of beta parapapillary atrophy, absence of beta atrophy with or without overhanging Bruch`s membrane, or uncertainty of presence was registered in all included degree sections and in total for right eye, left eye and both eyes. Uncertainty was defined as uncertain differentiation between the retinal pigment epithelium and Bruch`s membrane, or indistinguishable distal border, caused by other reasons than the exclusion criteria.

3.5.3.3   Gamma parapapillary atrophy

Gamma parapapillary atrophy was for the purpose of this study defined as an area devoid of choroid, seen as an irregular hypo- and hyperreflective area under Bruch`s membrane, Bruch`s membrane, seen as the lowermost hyperreflective line in the absence of retinal pigment epithelium, and deeper retinal layers, from and including the ganglion cell layer to the retinal pigment epithelium (Dai et al., 2013; Miki et al., 2017; Miki et al., 2019; Vianna et al., 2016; Zhang et al., 2018). In other terms, gamma parapapillary atrophy was defined as bare sclera with overlying retinal nerve fibre layer (figure 3-6). Gamma parapapillary atrophy was regarded as the area from the ending of an intact Bruch`s membrane to the border of the papilla, defined as the border tissue of Elschnig, as previously described. The gamma parapapillary atrophy was registered as

absent, present or uncertain about presence in all included degree sections and in total for right eye, left eye and both eyes. Uncertainty was defined as uncertain differentiation between Bruch`s membrane and the sclera, or indistinguishable distal border, caused by other reasons than the exclusion criteria.
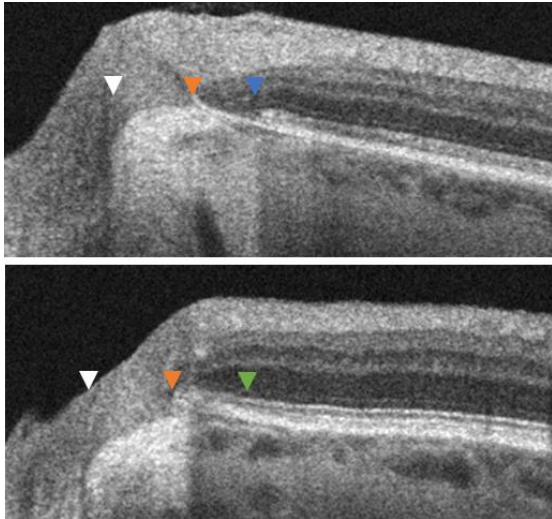
Figure 3-6: Gamma parapapillary atrophy. The OCT sections show gamma parapapillary atrophy between the ending of Bruch`s membrane (orange arrowhead) and the border tissue of Elschnig (white arrowhead). In the upper degree section, beta parapapillary atrophy is adjacent, between the ending of retinal pigment epithelium (blue arrowhead) and the ending of Bruch`s membrane. In the lower degree section, alpha is adjacent, between the gradual ending of IS-OS junction (green arrowhead) and the ending of Bruch`s membrane.

3.6 Statistics

The registration of demographic data was transferred into an Excel sheet for the DVOH-project by two master students (J.L.P., S.S), which was stored unavailable to other master student. The registrations from the degree sections were plotted into Excel (Microsoft Office 365 ProPlus, version 1808, 2019) from the manual registration form. These two datasets were merged into one complete dataset, by connecting them with the code key, which linked the journal number in the DVOH-project to the identification number in the current study (figure 3-7). All data in the dataset was doubled checked for errors before statistical analyses.
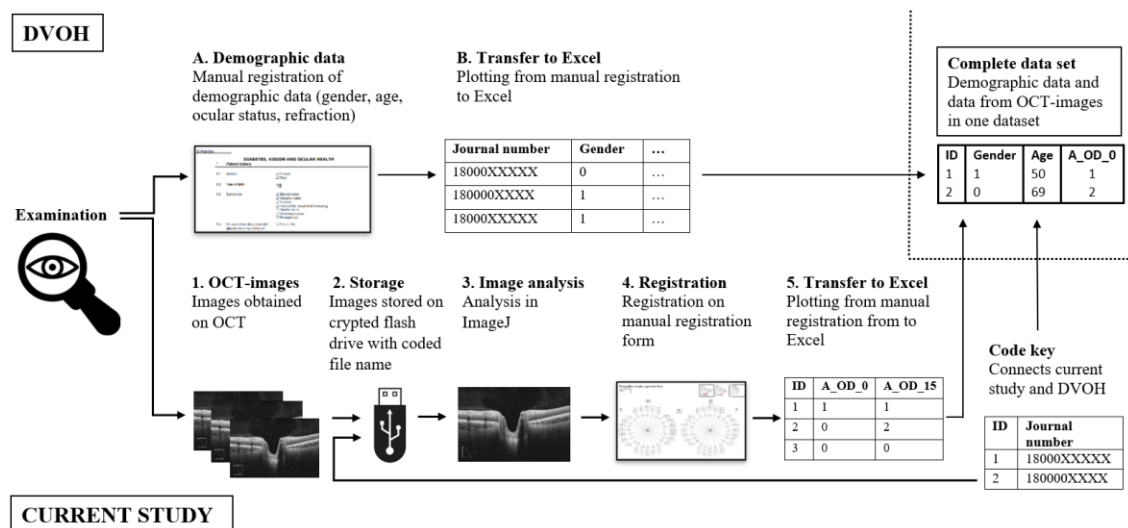
Figure 3-7*: Flow chart of data management.* The figure is a flow chart indicating the protocol from obtaining data in the examination to a complete dataset in Excel, separated into DVOH and current study.

3.6.1 Statistical analyses

The complete data set was transferred to SPSS (IBM SPSS Statistics, version 25, 2017) for statistical analyses. Descriptive analyses, in the form of frequency for nominal variables, and mean with standard deviation (SD) and range for continuous variables, was performed for demographic data. Descriptive analyses were also used for finding the frequency of alpha, beta and gamma parapapillary atrophy in each degree section and in total for each and both eyes. McNemar test was used for comparing the frequency between the right and left eyes. A significance level (p-value) of 0.05 was used. The frequencies of parapapillary atrophy were transferred to Excel, where the 95 percent confidence interval was calculated. Polar diagrams were made in Excel, with the frequencies and confidence intervals. The degree names (0, 15, 30…) of degree sections in the right eye, from the scan pattern, was mirrored for the analysis and polar diagrams, to ensure that each degree value represents the same location when referring to either eye, meaning that the 0 degree section always refers to temporal side and the 180 degree section always refers to nasal side.

3.6.2 Post-hoc analyses

Post-hoc analyses, in the form of descriptive analysis, was done in SPSS for the configuration of the ending of IS-OS junction, either gradual or abrupt, in presence of alpha parapapillary atrophy in a degree section, and for presence of overhanging

Bruch`s membrane in those without definitive beta in an degree section. Uncertain registrations were excluded from the post-hoc analyses.

3.7 Ethics

The subjects went through an extensive examination which lasted for approximately three hours, where the procedures for the current study was estimated to have a duration of 40 minutes, including a 20-minute break for effect of Tropicamide. The duration of the examination was thoroughly explained beforehand, and those who wanted shorter duration over several days, or needed to evacuate the examination, was accommodated. The subject was also given the possibility to ask for smaller breaks if necessary. All subjects signed a consent form and was not recognized as included in the study before this, and they were given multiple opportunities to ask questions and receive answers. Also, they were informed about the possibility to drop out of the study and withdrawal of consent, without further explanation, at any time.

The anonymity of the subject was a major concern in the presented study, and all information was handled with confidentiality. This was maintained mainly by giving the subjects a random identification number, which was used in all identification for the current study. The identification number and the identity of the subjects, in the form of a journal number, was contained in the code key, which was stored with restricted access in the research repository. All images and the data sets were stored on the crypted flash drive, where only the main observer had access. The manual registration forms with identification numbers, which were without personal information, was handled and stored safely by the main observer. The manual registration forms will be destroyed at the end of the study, at latest 31st of December 2019. The dataset and OCT sections, as well as the code key, will be given to the supervisors for further use in the DVOH-project.

All procedures were non-invasive and did not cause pain or severe discomfort. Tropicamide is a common tool in daily optometric practice and are known to cause temporary discomfort and blurred vision (Felleskatalogen, 2015). Serious complications or side effects are seldom in the use of these drops (Felleskatalogen, 2015). Information about the effect and duration of the diagnostic medicament was given, and the subjects

consented before installation. In addition, allergies, intraocular pressure and the anterior chamber angle was assessed in all subjects, to ensure safety of the use of Tropicamide. In regards of the OCT, it uses a laser to obtain the images. The laser is classified as Laser Class 1, meaning that it does not produce risk of injury for the subjects (Norwegian electrotechnical publication, 2014).

If there were findings during the examination that needed further management, the issue was addressed with the proper reaction, either further follow-up in the optometric clinic National Centre for Optics, Vision and Eye Care at the University of Southeast Norway or as a report or referral to another optometrist or ophthalmologist. The study was approved by the Regional Committees for Medical and Health Research Ethics and is in line with the Declaration of Helsinki.

4 Results

The composition of the study population is given in table 4-1. Ten (14.3 %) subjects had self-reported diabetic retinopathy, and 1 (1.4 %) subject reported another retinopathy. No subjects had age-related macular degeneration. Three (4.3 %) subjects had self-reported glaucoma, and 18 (25.7 %) subjects had cataract.

Variable	Subjects N = 70
Gender	34 (48.6 %) females 36 (51.4 %) males
Age	61.33 years ± 9.68 Range: 43, 81
Spherical power, right eyes	-0.05 DS ± 2.78 Range: -11.00, +8.25
Cylindrical power, right eyes	-0.88 DC ± 0.61 Range: -0.25, -3.50
Spherical power, left eyes	-0.17 DS ± 2.61 Range: -9.50, +7.00
Cylindrical power, left eyes	-0.91 DC ± 0.69 Range: -0.25, -4.50

Table 4-1: Demographic data of study population. The table summarizes characteristics of the study population. N=number of included subjects. DS = dioptres sphere. DC = dioptres cylinder. ± = Standard deviation.

4.1 Parapapillary atrophy

Of the 140 eyes from 70 subjects, 3 (4.3 %) right eyes and 2 (2.9 %) left eyes were excluded because of missing image or misalignment of the scan pattern outside the papilla. Therefore, the total number of eyes for analysis was 67 right eyes and 68 left eyes, with both eyes being represented in 65 subjects. Eighteen (26.9 %) right eyes had misalignment outside the central 20 percent of the papilla, causing 162 (20.2 %) OCT sections to be excluded. Twenty (29.4 %) left eyes had misalignment outside the central 20 percent of the papilla, causing 180 (22.1 %) OCT sections to be excluded. Therefore, the total number of included OCT sections for the right eyes was 642, representing 1284 degree sections, and the total number for left eyes was 636, representing 1272 degree sections. Further exclusion was based on each of the parapapillary atrophies in each degree section.

4.1.1 Alpha parapapillary atrophy

Out of the remaining 1284 degree sections of right eyes and 1272 degree sections of left eyes, 100 (3.8 %) and 120 (4.7%), respectively, were excluded based on inadequate image quality.

4.1.1.1 Frequency and distribution of frequencies of alpha parapapillary atrophy

The frequency and confidence interval for each degree section is given in table 4-2 and illustrated in chart 4-1. Alpha parapapillary atrophy was found in 67 (100 %) right eyes, 68 (100 %) left eyes, and were present in both eyes in 65 (100 %) subjects. The frequency of alpha parapapillary atrophy in the right eyes varied from 92.9 % (CI: 85.1, 100) in the 240 degree section to 100 % in the 30, 45, 120, 135, 150, 210, 315 and 330 degree sections. In the left eye, the frequency varied from 90.9 % (CI: 82.4, 99.4) in the 270 degree section to 100 % in the 0, 15, 90, 105, 135 and 330 degree sections.

Chart 4-1: *Polar diagrams regarding alpha parapapillary atrophy.* Polar diagrams showing the distributions of frequencies (percentages) of alpha parapapillary atrophy (green colour) along degree sections in right eyes (left illustration) and left eyes (right illustration). Values between degree sections were extrapolated. The stippled lines indicate 95 percent confidence interval. The rim of the sketched papilla corresponds to 0 percent, and each grey circle represents 20 percent increase.

4.1.2 Beta parapapillary atrophy

Out of the remaining 1284 degree sections of right eyes and 1272 degree sections of left eyes, 177 (6.9 %) and 206 (8.1 %), respectively, were excluded based on inadequate image quality.

4.1.2.1 *Frequency and distribution of frequencies of beta parapapillary atrophy*

Frequencies and confidence intervals for all degree sections can be seen in table 4-2 and are illustrated in chart 4-2. Beta parapapillary atrophy was found in 52 (77.6 %, CI: 67.6, 87.6) right eyes and 45 (66.2 %, CI: 55.9, 77.4) left eyes. The difference in prevalence between the eyes was not statistically significant (p = 0.118). The atrophy was present in both eyes in 39 (60.0 %, CI: 55.9, 77.4) subjects. In right eyes, beta parapapillary atrophy was most often found in the 345 degree section, with a frequency of 71.7 % (CI: 60.3, 83.1), and most rarely found in the 195 degree section with a frequency of 19.3 % (CI: 9.1, 29.5). In the left eyes, the frequency of 66.7 % (CI: 54.1, 79.3) in the 15 degree section was highest, and the frequency of 18.8 % (CI: 5.3, 32.3) in the 225 degree section was lowest.

Chart 4-2: *Polar diagrams regarding beta parapapillary atrophy.* Polar diagrams showing the distributions of frequencies (percentages) of beta parapapillary atrophy (blue colour) along degree sections in right eyes (left illustration) and left eyes (right illustration). Values between degree sections were extrapolated. The stippled lines indicate 95 percent confidence interval. The rim of the sketched papilla corresponds to 0 percent, and each grey circle represents 20 percent increase.

4.1.3 Gamma parapapillary atrophy

Out of the remaining 1284 degree sections of right eyes and 1272 degree sections of left eyes, 53 (2.1 %) and 59 (2.3 %), respectively, were excluded based on inadequate image quality.

4.1.3.1 *Frequency and distribution of frequencies of gamma parapapillary atrophy*

The frequencies and confidence intervals for all degree sections are given in table 4-2 and illustrated in chart 4-3. Gamma parapapillary atrophy was present in 15 (22.4 %, CI: 12.4, 32.4) right eyes and 15 (22.1 %, CI: 12.2, 32.0) left eyes. The difference in prevalence between the eyes was not statistically significant (p = 1.0). The atrophy was present in both eyes in 13 (20.0 %, CI: 10.3, 29.7) subjects. The highest frequency in right eyes was in the 345 degree section, with 23.3 % (CI: 12.6, 34.0), and it was not present at all in the degree sections of 90 through 225. In left eyes, the atrophy occurred most often in the 300 degree section, with a frequency of 22.4 % (CI: 10.7, 34.1), and was not present in the degree sections of 75 through 225.
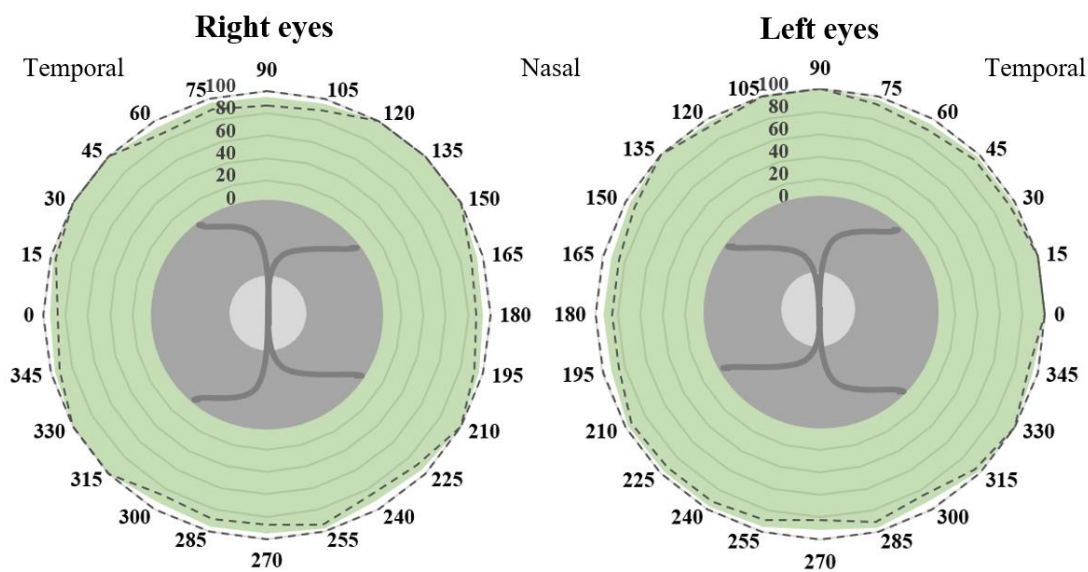

Chart 4-3: *Polar diagrams regarding gamma parapapillary atrophy.* Polar diagrams showing the distributions of frequencies (percentages) of gamma parapapillary atrophy (orange colour) along degree sections in right eyes (left illustration) and left eyes (right illustration). Values between degree sections were extrapolated. The stippled lines indicate 95 percent confidence interval. The rim of the sketched papilla corresponds to 0 percent, and each grey circle represents 20 percent increase.

Chart 4-4 illustrates the differences in distribution of frequencies between alpha, beta and gamma parapapillary atrophy, and table 4-2 shows frequency and 95 percent confidence intervals for each of the parapapillary atrophies in all degree sections and for each eye.
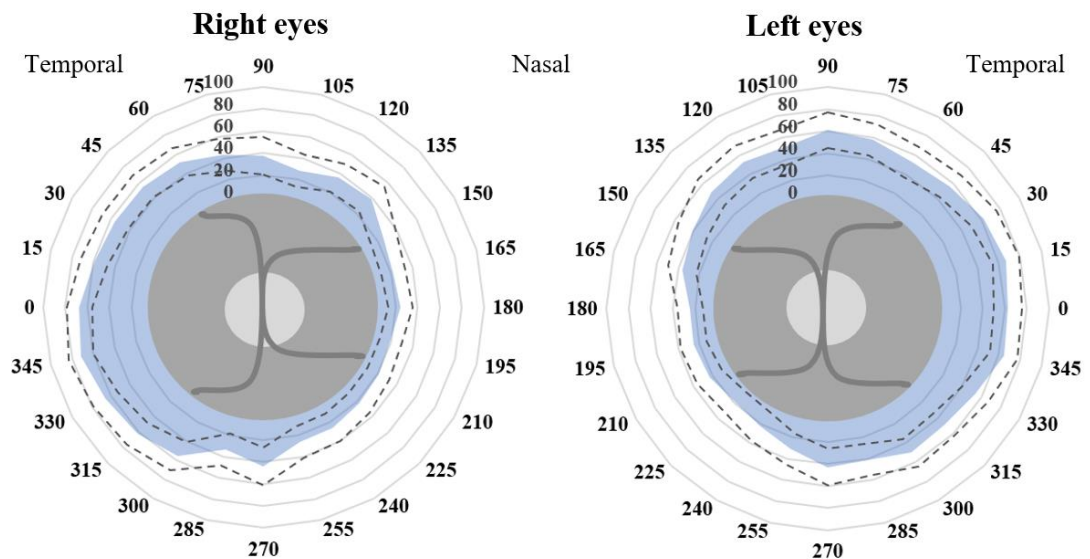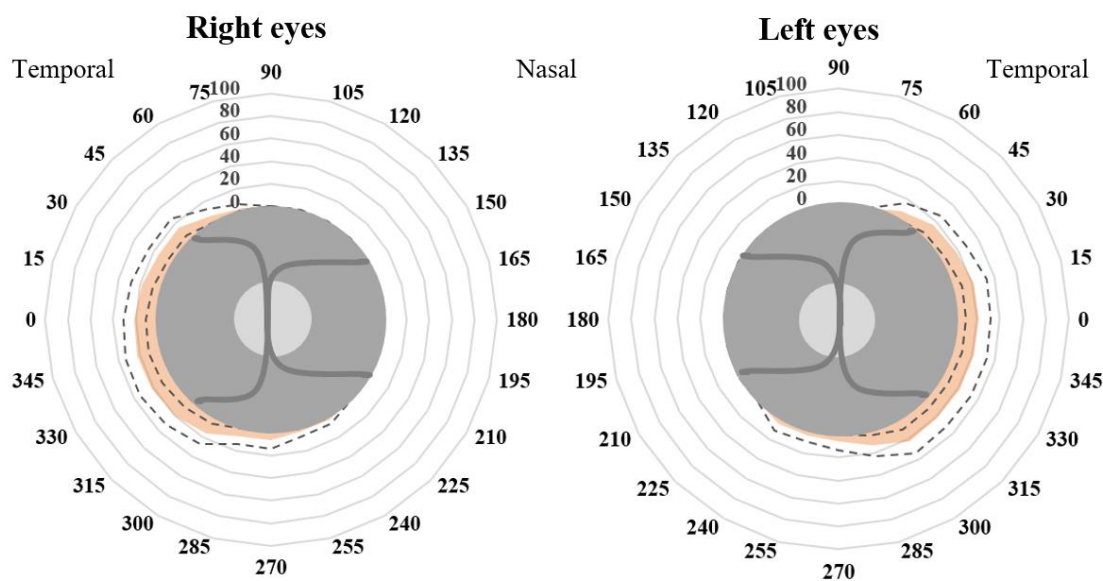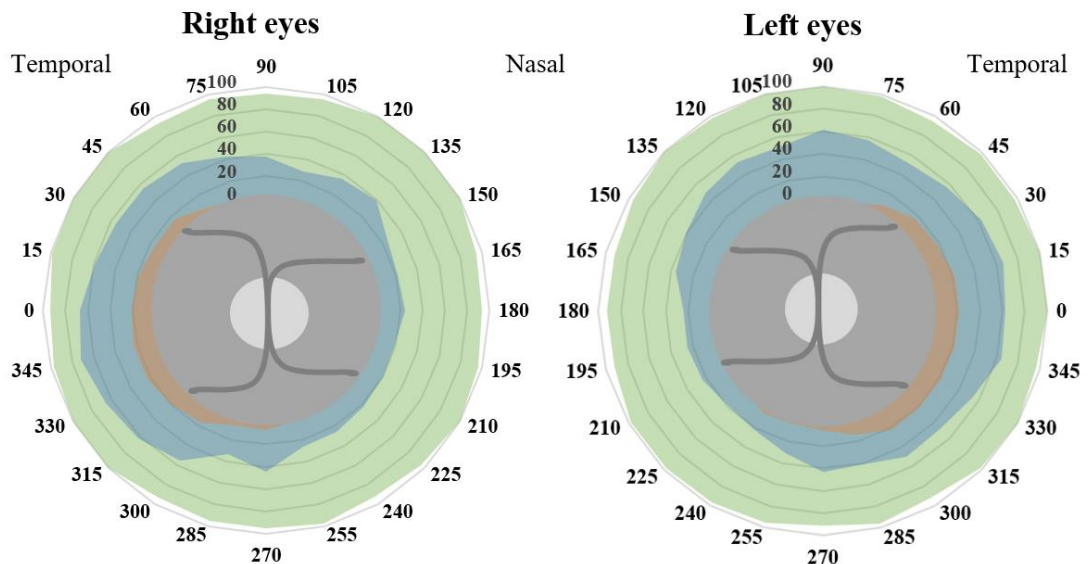

Chart 4-4: *Polar diagrams regarding all parapapillary atrophies.* Polar diagrams showing the distributions of frequencies (percentages) of alpha (green colour), beta (blue colour) and gamma (orange colour) parapapillary atrophy along degree sections in right eyes (left illustration) and left eyes (right illustration). Values between degree sections were extrapolated. The rim of the sketched papilla corresponds to 0 percent, and each grey circle represents 20 percent increase.

Degrees	RIGHT EYES			LEFT EYES		
	Alpha n/N (%) [CI]	**Beta** n/N (%) [CI]	**Gamma** n/N (%) [CI]	**Alpha** n/N (%) [CI]	**Beta** n/N (%) [CI]	**Gamma** n/N (%) [CI]
0	**58/62 (93.5)** [87.4, 99.6]	**41/61 (67.2)** [55.4, 79.0]	**13/62 (21.0)** [10.9, 31.1]	**56/56 (100)** [100, 100]	**35/56 (62.5)** [49.8, 75.2]	**12/56 (21.4)** [10.7, 32.1]
15	**58/59 (98.3)** [95.0, 100]	**35/59 (59.3)** [46.8, 71.8]	**11/59 (18.6)** [8.7, 28.5]	**55/55 (100)** [100, 100]	**36/54 (66.7)** [54.1, 79.3]	**12/55 (21.8)** [10.9, 32.7]
30	**52/52 (100)** [100, 100]	**29/52 (55.8)** [42.3, 69.3]	**8/52 (15.4)** [5.6, 25.2]	**50/51 (98.0)** [94.2, 100]	**32/51 (62.7)** [49.2, 76.0]	**9/52 (17.3)** [7.0, 27.6]
45	**51/51 (100)** [100, 100]	**28/51 (54.9)** [41.2, 68.6]	**8/51 (15.7)** [5.7, 25.7]	**50/51 (98.0)** [94.2, 100]	**28/50 (56.0)** [42.2, 69.8]	**8/50 (16.0)** [5.8, 26.2]
60	**45/48 (93.8)** [87.0, 100]	**25/48 (52.1)** [38.0, 66.2]	**3/48 (6.3)** [0, 13.2]	**43/45 (95.5)** [89.4, 100]	**23/44 (52.3)** [37.5, 67.1]	**4/49 (8.2)** [0.5, 15.9]
75	**45/47 (95.8)** [90.1, 100]	**18/42 (42.9)** [27.9, 57.9]	**1/49 (2.0)** [0, 5.9]	**45/46 (97.8)** [93.6, 100]	**26/45 (57.8)** [43.4, 72.2]	**0/51 (0)** [0, 0]
90	**34/36 (94.4)** [86.9, 100]	**12/32 (37.5)** [20.7, 54.3]	**0/44 (0)** [0, 0]	**39/39 (100)** [100, 100]	**22/36 (61.1)** [45.2, 77.0]	**0/51 (0)** [0, 0]
105	**40/42 (95.3)**	**10/35 (28.6)**	**0/51 (0)**	**44/44 (100)**	**20/39 (51.3)**	**0/51 (0)**

	[88.9, 100]	[13.6, 43.6]	[0, 0]	[100, 100]	[35.6, 67.0]	[0, 0]
120	45/45 (100) [100, 100]	15/42 (35.7) [21.2, 50.2]	0/47 (0) [0, 0]	44/45 (97.8) [93.5, 100]	19/36 (52.8) [36.5, 69.1]	0/46 (0) [0, 0]
135	40/40 (100) [100, 100]	14/36 (38.9) [23.0, 54.8]	0/46 (0) [0, 0]	47/47 (100) [100, 100]	16/33 (48.5) [31.5, 65.6]	0/50 (0) [0, 0]
150	49/49 (100) [100, 100]	11/43 (25.6) [12.6, 38.6]	0/50 (0) [0, 0]	48/50 (96.0) [90.6, 100]	18/44 (40.9) [26.4, 55.4]	0/51 (0) [0, 0]
165	55/58 (94.8) [89.1, 100]	12/55 (21.8) [10.9, 32.7]	0/59 (0) [0, 0]	47/51 (92.2) [84.8, 99.6]	18/50 (36.0) [22.7, 49.3]	0/54 (0) [0, 0]
180	56/60 (93.4) [87.1, 99.7]	14/58 (24.1) [13.1, 35.1]	0/61 (0) [0, 0]	49/53 (92.4) [85.3, 99.5]	13/53 (24.5) [12.9, 36.1]	0/55 (0) [0, 0]
195	57/59 (96.6) [92.0, 100]	11/57 (19.3) [9.1, 29.5]	0/59 (0) [0, 0]	47/51 (92.2) [84.8, 99.6]	13/51 (25.5) [13.5, 37.5]	0/53 (0) [0, 0]
210	52/57 (100) [100, 100]	10/49 (20.4) [9.1, 31.7]	0/52 (0) [0, 0]	48/49 (98.0) [94.1, 100]	10/43 (23.3) [10.7, 35.9]	0/49 (0) [0, 0]
225	46/47 (95.7) [90.0, 100]	9/40 (22.5) [9.6, 35.4]	0/48 (0) [0, 0]	36/37 (97.3) [92.1, 100]	6/32 (18.8) [5.3, 32.3]	0/45 (0) [0, 0]
240	39/42 (92.9) [85.1, 100]	9/35 (25.7) [11.2, 40.1]	1/46 (2.2) [0, 6.4]	35/36 (97.2) [91.8, 100]	6/27 (22.2) [6.5, 37.9]	2/40 (5.0) [0, 11.8]
255	45/46 (97.8) [93.6, 100]	9/34 (26.5) [11.7, 41.3]	1/45 (2.2) [0, 6.5]	42/44 (95.5) [89.4, 100]	12/39 (30.8) [16.3, 45.3]	2/48 (4.2) [0, 9.9]
270	36/38 (94.7) [87.6, 100]	15/34 (44.1) [27.4, 60.8]	3/44 (6.8) [0, 14.2]	40/44 (90.9) [82.4, 99.4]	15/35 (42.9) [26.5, 59.3]	3/47 (6.4) [0, 13.4]
285	41/43 (95.3) [89.0, 100]	12/36 (33.3) [17.9, 48.7]	3/46 (6.5) [0, 13.6]	48/50 (96.0) [90.6, 100]	18/44 (40.9) [26.4, 55.4]	7/52 (13.5) [4.2, 22.8]
300	42/45 (93.3) [86.0, 100]	25/45 (55.6) [41.1, 70.1]	8/49 (16.3) [6.0, 26.6]	46/50 (92.0) [84.5, 99.5]	23/46 (50.0) [35.6, 64.4]	11/49 (22.4) [10.7, 34.1]
315	50/50 (100) [100, 100]	31/50 (62.0) [48.5, 75.5]	10/50 (20.0) [8.9, 31.1]	51/52 (98.0) [94.2, 100]	25/52 (48.1) [34.5, 61.7]	11/52 (21.2) [10.1, 32.3]
330	53/53 (100) [100, 100]	35/53 (66.0) [53.2, 78.8]	12/53 (22.6) [11.3, 33.9]	52/52 (100) [100, 100]	28/52 (53.8) [40.2, 67.4]	11/52 (21.2) [10.1, 32.3]
345	58/60 (96.6) [92.0, 100]	43/60 (71.7) [60.3, 83.1]	14/60 (23.3) [12.6, 34.0]	52/54 (96.3) [91.3, 100]	35/54 (64.8) [52.1, 77.5]	12/55 (21.8) [10.9, 32.7]
Total	67/67 (100) [100, 100]	52/67 (77.6) [67.6, 87.6]	15/67 (22.4) [12.4, 32.4]	68/68 (100) [100, 100]	45/68 (66.2) [55.9, 77.4]	15/68 (22.1) [12.2, 32.0]

Table 4-2: *Frequencies of alpha, beta and gamma parapapillary atrophy.* The table shows the frequency and 95 percent confidence interval for alpha, beta and gamma parapapillary atrophy for all degree sections and in total for either eye. N = number of included eyes, n = number of eyes with atrophy, CI = confidence interval.

4.2 Post-hoc analyses

4.2.1 Frequencies of gradual and abrupt ending of IS-OS junction

Both gradual and abrupt endings of IS-OS junction was observed in OCT sections with alpha parapapillary atrophy (details in Annex 4). In right eyes, the presence of gradual endings occurred most often, with a prevalence of 100 %, in the 45, 120, 135, 225, 255,

270 and 285 degree sections. The degree section with the least prevalence of gradual endings was the 90 degree section with 91.2 % of right eyes. These frequencies are reverse for abrupt endings in the same degree section. In most degree sections (17 of 24) in right eyes, the frequency for gradual endings were equal to or higher than 95.0 %, and likewise under 5.0 % for abrupt endings. For left eyes, the presence of a gradual ending of the IS-OS junction in OCT sections with alpha parapapillary atrophy, varied from 85.7 % in the 0 degree section to 100 % in the 75, 90, 135, 210, 240, 255 and 285 degree sections. Therefore, the gradual endings were least frequent, and abrupt endings most frequent, in the 0 degree section. In left eyes, most degree sections (17 of 24) had a frequency of gradual endings equal to or above 95.0 %.

4.2.2 Frequencies of overhanging Bruch`s membrane

The frequencies for all degree sections are given in table 4-3 (details in Annex 5). Overhanging Bruch`s membrane was only registered for those without beta parapapillary atrophy, meaning in 15 (22.4 %) right eyes and 23 (33.8 %) left eyes. The presence varied from 4.2 percent in the 285 degree section to 34.4 percent in the 150 degree section, in right eyes. In left eyes, the prevalence varied from 0 percent in the 0 degree section to 52.9 percent in the 135 degree section. The high and low frequencies in the parapapillary retina is scattered. Most sections in both eyes has a prevalence between 20 and 30 percent, some are below 20 percent, and a few are above 30 percent.

5 Discussion

In the presented study, the main purpose was to estimate the prevalence and distribution of alpha, beta and gamma parapapillary atrophy as identified by the means of SD-OCT.

5.1 Alpha parapapillary atrophy

5.1.1 Prevalence of alpha parapapillary atrophy in one and both eyes

In this study, alpha parapapillary atrophy was found to be present in 100 percent of right and left eyes. This coincides with the finding of Lee et al (2010), the only OCT study that has included alpha parapapillary atrophy. Although the literature is sparse regarding alpha parapapillary atrophy seen in OCT sections, the ophthalmoscopic alpha parapapillary atrophy has been extensively studied. Therefore, it seems appropriate to see how the prevalence from the current study compares to the ophthalmoscopically reported prevalence in normal eyes.

There are variations in the frequencies reported from ophthalmoscopic studies, with the highest being 98.6 percent of eyes from Jonas et al (2003), and the lowest being 58.0 percent of eyes from Ramrattan et al (1999). Other studies have found a prevalence of 84.4 percent and 71.2 percent (Jonas et al., 1989; Wang et al., 2008). These differences might be explained by differences in the study population, such as age, number of subjects, difference in refractive errors and ethnicity (Jonas et al., 1989; Jonas et al, 2003; Ramrattan et al, 1999; Wang et al., 2008). One could also assume that there have been some developments in the fundus cameras used in the different studies, given the time of studies is spread over 19 years. Either way, there seems to be a difference between the current study and the ophthalmoscopic studies, which could be factual since the definition of the atrophy on the two imaging techniques is different.

The higher frequency of alpha parapapillary atrophy on OCT sections compared to ophthalmoscopically might be caused by the fact that the definition used in the current study and by Lee et al (2010) is not the same as the histologic definition of alpha parapapillary atrophy. The histologic definition has been proven to be highly correlated with the ophthalmoscopic definition (Kubota et al., 1993). Therefore, it is possible that the definition in OCT sections as used in the presented study do not reflect the atrophy

seen ophthalmoscopically or histologically. However, there has yet to be proven in a study that the histologic findings of alpha, meaning cellular changes in the retinal pigment epithelium, can be seen in OCT sections with the current resolution of the instruments (Lee et al., 2010). There are studies that has demonstrated alpha parapapillary atrophy by the histologic definition in illustrations in their studies, even though the changes in the retinal pigment epithelium cannot be easily seen in the illustrations (Dai et al., 2013; Jonas et al., 2015). Further research should be executed to develop a common definition for alpha parapapillary atrophy, which correlates with the atrophy seen ophthalmoscopically. The suspicion of alpha parapapillary atrophy being of limited diagnostic value is strengthened by the current study, since the prevalence of 100 percent, in one eye and both, might insinuate that alpha parapapillary atrophy is a natural change related to age (Ramrattan et al., 1999). However, it is important to separate the atrophy from other conditions, such as hypertrophy of the retinal pigment epithelium, which is also ophthalmoscopically seen as hyperpigmentation (Kubota et al., 1999; Ramrattan et al., 1999).

The prevalence of alpha parapapillary atrophy in both eyes was 100 percent in the current study. There are no OCT studies to compare this prevalence with. Studies that has included both eyes of the subject, reports the prevalence in at least one eye, and not for both eyes of a subject (Jonas et al., 2003; Ramrattan et al., 1999; Wang et al., 2008). The prevalence of alpha parapapillary atrophy when using OCT should be further studied, both in one and both eyes. It is important to know how often alpha parapapillary atrophy is present in an eye, and to know the likelihood of the atrophy to be present in both eyes of one subject.

5.1.2 Distribution of frequencies of alpha parapapillary atrophy

To my knowledge, there has been no studies using OCT to investigate the distribution alpha parapapillary atrophy most frequently occurs in. The study mentioned previously, by Lee et al (2010) only investigated the temporal horizontal region, between 8 and 10 o`clock in right eyes, interpreted as between the 330 and 30 degree sections of both eyes in the current study. They reported a prevalence of 100 percent. In this area in the current study, the prevalence varies between 93.5 and 100 percent in right eyes and between 98.0 to 100 percent in left eyes. Therefore, the frequencies found in the

previous and presented study seems to coincide relatively well. There is no apparent reason for why the lowest temporal prevalence in right eyes varies 6.5 percent from that of Lee et al (2010) and 4.5 percent from that of the left eyes. One should reflect upon the definition used in the studies, which are the same in the two studies, because it might not be interpreted in the same manner. To estimate the distribution of frequency more accurately, larger population-based studies should be conducted.

There does not seem to be a specific pattern of how the frequencies of alpha parapapillary atrophy are distributed in the parapapillary retina, which contradicts the ophthalmoscopic studies which has found that the prevalence was higher temporally (between 2 and 4 o`clock in a left eye), compared to inferiorly (between 4 and 7 o`clock in a left eye), followed by superiorly (between 11 and 2 o`clock in a left eye), and rarely nasally (between 11 and 7 o`clock in a left eye) (Jonas et al., 1989; Jonas et al., 2003; Wang et al., 2008). It can, however, be argued that the prevalence in the presented study is lower around the horizontal and vertical midlines in right eyes, and in the nasal and inferior areas of left eyes (chart 4-1). There has not been done significance testing regarding the differences between the sections, for any of the parapapillary atrophies, since this was regarded as exceeding the main purpose of the study and would require extensive statistical analyses. Because of the small variations in prevalence between the degree sections in both eyes, it cannot be concluded, based on the current study, that there is difference of frequencies between the different areas surrounding the papilla.

5.2 Beta parapapillary atrophy

5.2.1 Prevalence of beta parapapillary atrophy in one and both eyes

The prevalence of beta parapapillary atrophy in the current study was 77.6 percent of right eyes and 66.2 percent of left eyes. There was not a significant difference in the prevalence between the eyes, which is what we generally expect. Compared to other studies regarding beta parapapillary atrophy using SD-OCT in normal eyes, the frequencies are somewhat similar. Lee et al (2010) found a prevalence of 75.0 percent in at least one eye, and Hayashi et al (2012) reported 63.0 percent in at least one eye. New research from Zhang et al (2018) detected beta parapapillary atrophy in 72.6 percent of eyes. The prevalence in right eyes in the current study is a little higher than

previous studies, and the prevalence in left eyes in the current study is in the middle of the previously reported frequencies.

The are several similarities between the current and previous studies, which indicates that a similar prevalence is expected. All studies have used SD-OCT, meaning the same generation of OCTs, although the exact instrument is not necessarily the same. The age of the subjects is quite similar, with the previous studies having an average of mid- to high fifties compared to 61 years in current study (table 4-1) (Hayashi et al., 2012; Lee et al., 2010; Zhang et al., 2018). A higher age in the study population could increase the prevalence of beta parapapillary atrophy (Kim et al., 2013; Wang et al., 2008; Zhang et al., 2018). The mean refractive errors in the previous studies seem to be a bit more in the minus direction, but they use spherical equivalent, meaning that a higher amount of minus can be expected (Hayashi et al., 2012; Lee et al., 2010; Zhang et al., 2018). There has been found a slight association between the presence of beta parapapillary atrophy and myopia, in the sense that increased myopia could provide higher frequency of beta (Wang et al., 2008; Zhang et al., 2018). Two of the studies, Hayashi et al (2012) and Lee et al (2010) are, as the current study, relatively small with a study population of 100 and 120 eyes, respectively, whilst Zhang et al (2018) is a larger study with 723 eyes. Hayashi et al (2012), which is the study with the most different prevalence from the others, has lower prevalence of men, which has been suggested to have a correlation to lower prevalence of beta parapapillary atrophy by Zhang et al (2018). In conclusion, the prevalence from the right eyes seems to be most similar to the findings of Lee et al (2010), whilst the prevalence from the left eyes are most similar with the findings of Hayashi et al (2012). These two are also the most equal to the current study, even though the demographics are similar for all, because of the number of eyes included in the study. Lastly, it is interesting that the frequencies, both from current and previous studies, are much higher than those that has been found ophthalmoscopically, which varies between 11.4 and 19.9 percent (Jonas et al, 1989; Jonas et al., 2003; Ramrattan et al., 1999; Wang et al., 2008).

The prevalence of beta parapapillary atrophy in both eyes of subjects was 60.0 percent, meaning lower than reported for either right or left eyes. There are currently no other studies that has reported the prevalence of subjects with beta parapapillary atrophy present in both eyes. The difference is clinically relevant, because the lower prevalence

found in both eyes, compared to one eye, suggest that the atrophy can be expected to be present in only one eye in some subjects. It would have been interesting with further studies researching if there are associations which explains the presence in one compared to both eyes. Associations between prevalence of atrophy and demographic data was outside the scope of the study.

5.2.2 Distribution of frequencies of beta parapapillary atrophy

The distributions of frequencies are relatively symmetrical between the eyes. The prevalence is lower in the nasal or inferonasal area, and increasing towards the inferior and superior regions, and reaching a peak in the temporal area. The frequencies seem to have an even increase and decrease in the parapapillary retina, seen as the smooth curve of the blue colour in the polar diagram, apart from in the 285 degree section in the right eyes, which caused a clear inward notch in this area. The frequencies seem to tend to be higher in the superior area of the left eyes, and in the inferotemporal region of the right eyes, when compared with each other.

The distribution of frequency of beta parapapillary atrophy has been previously investigated by Zhang et al (2018). They reported that beta parapapillary atrophy was found frequently in the temporal area and rarely nasally, which is supported by the findings in the current study. They describe the parapapillary area in sectors, however, they do not inform how the sectors are distributed in the area, but it is interpreted that they correspond to the horizontal and vertical midlines of the papilla, meaning temporally is equal to the 0 degree section, inferior to the 270 degree section, superior to the 90 degree section and nasal to the 180 degree section. In these areas they found the prevalence to be 87.4 percent of eyes temporally, 7.8 percent inferiorly, 4.8 percent superiorly and 0 percent nasally (Zhang et al., 2018). These percentages cannot be directly compared to those of the presented study, since the presented study did not exclude those without beta parapapillary atrophy from the statistical analyses. However, the percentages from both studies provide the same information. Both studies do find the prevalence to be highest temporally. Regarding the prevalence found superior and inferior, Zhang et al (2018) reports it to be higher inferiorly, which coincide with the right eyes in current study. In the left eyes in the current study, on the other hand, the opposite was found, with a difference of 19.6 percent related to the right eyes. The

results from the studies also differ in the nasal area, where Zhang et al (2018) had no eyes with beta parapapillary atrophy, whilst the present study found 24.1 and 24.5 percent of right and left eyes, respectively, which constitute 14 and 13 subjects respectively.

There is no apparent reason for why there should be a difference between the two studies regarding inferior and superior in left eyes, or nasally in both. Zhang et al (2018) had a mean age of 59.5 years and mean refractive power of spherical equivalent of -0.97 dioptres sphere, which is relatively equal to the current study (table 4-1). However, they have excluded eyes with ocular disease, such as glaucoma and diabetic retinopathy, which the presented study has not. In the case of glaucoma, which is associated with presence of beta parapapillary atrophy, there are not enough subjects with the disease in the current study that alone can account for the nasal frequencies of beta parapapillary atrophy (Hayashi et al., 2012; Jonas et al., 1989; Zhang et al., 2018). It is unknown how other ocular diseases might contribute to the difference in distribution of frequencies. Zhang et al (2018) did find an association of the prevalence of beta parapapillary atrophy and male gender, and there are a larger percentage of males in the current study than in the previous, which perhaps could have influenced the different findings. It should also be reflected upon that Zhang et al (2018) reports frequencies of just four degree sections, and there might be beta parapapillary atrophy, or a higher prevalence of beta, relatively close on either side of these four degree sections. The estimate of frequencies in different parapapillary areas from Zhang et al (2018) should be reliable, because of the high number of participants. However, the current study enlightens a much larger area of the parapapillary retina, and therefore might provide more accurate information. In ophthalmoscopic studies that has described beta parapapillary atrophy to be present in the same distribution as Zhang et al (2018), they reported presence of beta nasally, which coincide with the current study (Jonas et al, 1989; Jonas et al., 2003; Wang et al., 2008).

5.3 Gamma parapapillary atrophy

5.3.1 Prevalence of gamma parapapillary atrophy in one and both eyes

In the current study, the prevalence of gamma parapapillary atrophy was 22.4 percent in right eyes and 22.1 percent in left eyes. The difference between the eyes was found to be insignificant. As mentioned initially, there are just one previous study that has investigated the prevalence of gamma parapapillary atrophy specifically using OCT, although there are two additional studies that has found the prevalence of the atrophy, before the classification of gamma was developed (Hayashi et al., 2012; Lee et al., 2010; Zhang et al., 2018). The frequencies found in the current study differs from that found by Lee et al (2010) of 5.0 percent. Compared to the two other studies, by Hayashi et al (2012) and Zhang et al (2018) with frequencies of 28.0 and 26.3 percent, respectively, the prevalence found in the current study seems to concur, even though it is a bit lower.

The main cause for Lee et al (2010) being so different from the other studies, might be that the study did not specifically research the prevalence of gamma parapapillary atrophy, since the classification was yet to be developed. Their finding of a step configuration has only later been interpreted as gamma by Dai et al (2013) and Jonas et al (2012). On the other hand, this is also the case for Hayashi et al (2012), and their prevalence is like that of Zhang et al (2018) and the current study. Hayashi et al (2012) did however specify their finding as a defect of Bruch`s membrane and may correlate better to the definition of gamma parapapillary atrophy than the step configuration of the scleral bed reported by Lee et al (2010). Otherwise, one difference that separates Lee et al (2010) from the others, is the range of refractive power in the study population. The highest myopia in the study of Lee et al (2010) was -5.5 dioptres, compared to -11.0 dioptres sphere in the current study and -12.0 dioptres in the study of Zhang et al (2018). Hayashi et al (2012) did not specify the range of refractive errors in the study population. Presence of gamma parapapillary atrophy has been found to be significantly associated with myopia, and the prevalence has a steep increase after approximately -8.00 dioptres sphere (Dai et al., 2013; Jonas et al., 2012; Kim et al., 2013; Miki et al., 2017; Zhang et al., 2018).

There are no other studies reporting the prevalence of gamma parapapillary atrophy in both eyes. In the current study, gamma parapapillary atrophy was present in both eyes in 20.0 percent of subjects. If the percentages are specified into subjects, there were 15 subjects with gamma parapapillary atrophy in either the right or left eye, and there were 13 subjects who had the atrophy in both eyes. One of the two missing from the total for both eyes had exclusion of one of the eyes, and therefore there was one subject that did not have gamma parapapillary atrophy in both eyes. It would be interesting to see if the prevalence of those with gamma parapapillary atrophy in one eye would be higher in a larger population-based study.

5.3.2 Distribution of frequencies of gamma parapapillary atrophy

The distribution of frequencies starts supratemporal at 60 and 75 degrees in the right and left eyes, respectively, and has a steady increase towards the temporal and inferior area, which has a relatively even frequency throughout the area with a peak inferotemporally, before having a smooth decrease towards the inferonasal part. The distribution of frequencies in right and left eyes seems almost identical.

Zhang et al (2018) executed an investigation of the parapapillary retina, and found that gamma was found most frequently temporally and rarely nasally. As mentioned, the exact percentages from Zhang et al (2018) and the presented study cannot be directly compared, since the statistical analyses are different, however, both studies provides the same information. As previously, the sectors used by Zhang et al (2018) can be interpreted as the horizontal and vertical midlines of the papilla, meaning temporal is equal to the 0 degree section, inferior to the 270 degree section, superior to the 90 degree section and nasal to the 180 degree section. They found the prevalence of 52.1 percent temporally, 43.7 percent inferiorly, 2.6 percent superiorly and 1.6 percent nasally (Zhang et al., 2018). Therefore, it seems like the two studies agrees on the distribution of frequencies of gamma parapapillary atrophy, although the presented study did not have subjects with gamma parapapillary atrophy present superiorly or nasally. The fact that Zhang et al (2018) had low frequencies superiorly and nasally, and the current study had no subjects with the atrophy in these areas, might be caused by the higher number of subjects in the study. This is the most likely cause, since all other

demographic data is similar, and the percentages from Zhang et al (2018) represents only 5 eyes superiorly and 3 eyes nasally.

5.4 Summarization of parapapillary atrophies

Alpha parapapillary atrophy occurs most commonly of the parapapillary atrophies, followed by beta parapapillary atrophy, and at last gamma parapapillary atrophy. Although there was no significance testing regarding the differences between the atrophies, it is indicated that there is a relevant difference between them. Previous studies have also reported that alpha occurs significantly more often than beta parapapillary atrophy (Jonas et al., 1989; Jonas et al., 2003). It should also be noted that the atrophies look fairly symmetrical between the eyes, with some variations for beta parapapillary atrophy. The distribution of frequencies of beta and gamma parapapillary atrophy is similar, corresponding to the findings of Zhang et al (2018). There were no degree sections in all the 135 included eyes that had beta parapapillary atrophy without presence of alpha parapapillary atrophy in the same degree section. This coincides with the previous research which shows that these two atrophies are significantly associated with each other, meaning that beta is seldom present without alpha (Jonas et al., 2003). Regarding beta and gamma parapapillary atrophy, on the other hand, there were several degree sections where gamma parapapillary atrophy was present without beta parapapillary atrophy, as illustrated in figure 3-6. This has been reported before, and it has been found that these two atrophies do not occur directly dependent on each other (Dai et al., 2013; Vianna et al., 2016). Interestingly, there was a difference in exclusion between the parapapillary atrophies in the degree sections, where gamma parapapillary atrophy had least exclusion, followed by alpha parapapillary atrophy, and at last beta parapapillary atrophy. The possible cause might be the characteristics of the atrophies, since the bare sclera characterizing gamma parapapillary atrophy is easier to see than the separation of the RPE/BM-complex or the end of retinal pigment epithelium, which characterizes beta parapapillary atrophy.

5.5 Findings from post-hoc analyses

5.5.1 Frequency of gradual and abrupt ending of IS-OS junction

The frequencies of gradual endings found in the present study is generally higher than that of Lee et al (2010) of 86.7 percent, except for the 0 degree section in left eyes, which was 85.7 percent. The lower prevalence of gradual endings in this degree section seems reasonable because the prevalence of beta parapapillary atrophy is high in this section, and abrupt endings should therefore be more common, according to Lee et al (2010). However, beta parapapillary atrophy is frequently present in degree sections with a high prevalence, even 100 percent, of gradual endings and therefore it cannot be concluded, on the basis of the presented study, that there is an obvious connection between an abrupt ending of IS-OS junction and the presence of beta. It can, on the other hand, be concluded that both configurations of the ending were observed both in degree sections with and without beta parapapillary atrophy, and gradual endings were much more frequent than abrupt endings in all degree sections.

5.5.2 Frequency of overhanging Bruch`s membrane

In their study, Reis et al (2012) found overhanging Bruch`s membrane in most normal eyes, and the prevalence was highest in the superior and nasal quadrants. Reis et al (2012) found a relatively even curve of frequencies in normal eyes that was highest nasally, with 100 percent, followed by a slow decrease towards superior and temporal areas, to roughly 75 percent temporally, before dropping drastically below 50 percent inferiorly, and with a steep increase towards the nasal area again. In the present study, there does not seem to be similar findings. The prevalence does not exceed 34.4 and 52.9 percent, although it does coincide with the approximate location to the highest frequencies found by Reis et al (2012). The lowest frequencies in the presented study is found temporally and inferiorly, like Reis et al (2012). However, there are also some higher frequencies in the same area. Generally, the frequencies seem to be quite scattered in the parapapillary area in the current study, but with a tendency to be higher superior and nasally, meaning it concurs with Reis et al (2012).

5.6 Limitations of the current study

There are several limitations in the current study. First, there were many exclusions of OCT sections based on misalignment, and this was the highest cause of exclusion. These exclusions have caused the 95 percent confidence interval to increase. This issue might be partly due to five different master students being involved in the examination, and the issue could have been more restricted if there had been better training of the protocol in advance of the data collection, and better supervision by the main observer during the collection. Second, it should be mentioned that the ocular diseases reported in demographic data are self-reported from the subjects, meaning they could have diseases they are not aware of, causing the demographic data in this study to be wrong. Third, there might have been a learning effect in the analysis of the images that should to be discussed. In the beginning analyses, the knowledge and interpretation were likely different than in the end of the process. To compensate for this, analyses were performed twice, and the second registration of the images was used for the study. However, there are no assurances that the learning effect has not influenced the results. Intraobserver variation would provide further information about the variability in the interpretation of the parapapillary area within the main observer, but this was unfortunately not done (Dawson & Trapp, 2004). It would also have been advantageous to have an assessment of the interobserver variation, which would have indicated the variation in the interpretation of the parapapillary retina between the main observer and a second observer (Dawson & Trapp, 2004).

6 Conclusion

The prevalence of alpha parapapillary atrophy was 100 percent in either eye, and in both eyes of subjects. The distribution of frequencies was even around the parapapillary retina, with frequencies above 90 percent in all areas. The prevalence of beta parapapillary atrophy was 77.6 percent in right eyes, 66.2 percent in left eyes and 60 percent in both eyes. The atrophy occurred most often in the temporal region, followed by either superior or inferior, dependent on eye, and was least frequent in the nasal region. Gamma parapapillary atrophy was present in 22.4 percent of right eyes, 22.1 percent of left eyes and 20 percent in both eyes. Gamma parapapillary atrophy was most frequently present temporally and inferiorly, and was absent in the superior and nasal area.

The findings in this study seems to corroborate with previous studies concerning parapapillary atrophies and provides further information regarding prevalence and distribution, which should be beneficial in clinical practice. A unique finding in the current study include that alpha parapapillary atrophy is extremely common in the whole parapapillary retina, both in one and both eyes. Additionally, the study shows that beta parapapillary atrophy can be present in the nasal area, and that it can vary whether the prevalence is higher inferiorly or superiorly. Another interesting finding is that the prevalence of both beta and gamma parapapillary atrophy is higher in one eye of subjects than in both, suggesting that the atrophies might occur in only one eye of a subject. This is also the only known study that has found the prevalence and the distribution of all three parapapillary atrophies as identified by the means of SD-OCT in the same study population.

References

Carl Zeiss Meditec (2014) *Cirrus HD-OCT, Models 500 and 5000 – Documentation set* [user manual]

Curcio, C.A., Saunders, P.L., Younger, P.W. & Malek, G. (2000) Peripapillary Chorioretinal Atrophy – Bruch`s membrane Changes and Photoreceptor Loss. *Ophthalmology,* 107 (7), 334-343. DOI: 10.1016/S0161-6420(99)00037-8

Dai, Y., Jonas, J.B., Huang, H., Wang, M. & Sun, X. (2013) Microstructure of Parapapillary Atrophy: Beta Zone and Gamma Zone. *Investigative Ophthalmology & Visual Science,* 54 (3), 2013-2018. DOI: 10.1167/ivos.12-11255

Dawson, B. & Trapp, R.G. (2004) *Basic & Clinical Biostatistics* (4th edition). New York: Lange Medical Books/McGraw-Hill. ISBN: 0071410171

Dichtl, A., Jonas, J.B. & Naumann, G.O.H (1998) Histomorphometry of the optic disc in highly myopic eyes with absolute secondary angle closure glaucoma. *British Journal of Optometry,* 82 (3), 286-289. DOI: 10.1136/bjo.82.3.286

Felleskatalogen (2015) Tropikamid Minims. Available from: https://www.felleskatalogen.no/medisin/tropikamid-minims-bausch-&-lomb-u-k-ltd-564867 [30.03.2019]

Guo, Y., Wang, Y.X., Xu, L. & Jonas, J.B. (2012) Five-Year Follow-Up of Parapapillary Atrophy: The Beijing Eye Study. *PLoS ONE,* 7 (5), e32005. DOI: 10.1371/journal.pone.0032005

Hayashi, K., Tomidokoro, A., Lee, K.Y.C., Konno, S., Saito, H., Mayama, C., Aihara, M., Iwase, A. & Araie, M. (2012) Spectral-Domain Optical Coherence Tomography of β-zone Peripapillary Atrophy: Influence of Myopia and Glaucoma. *Investigative Ophthalmology & Visual Science,* 53 (3), 1499-1505. DOI: 10.1167/ivos.11-8572

Jonas, J.B., Jonas, S.B., Jonas, R.A., Holbach, L., Dai, Y., Sun, X. & Panda-Jones, S. (2012) Parapapillary Atrophy: Histological Gamma Zone and Delta Zone. *PLoS ONE,* 7 (10), e47237. DOI: 10.1371/journal.pone.0047237

Jonas, J.B., Jonas, S.B., Jonas, R.A., Holbach, L. & Panda-Jones, S. (2011) Histology of the Parapapillary Region in High Myopia. *American Journal of Ophthalmology,* 152 (6), 1021-1029. DOI: 10.1016/j.ajo.2011.05.006

Jonas, J.B., Nguyen, X.N., Gusek, G.C. & Naumann, G.O.H. (1989) Parapapillary Chorioretinal Atrophy in Normal and Glaucoma Eyes – I. Morphometric Data. *Investigative Ophthalmology & Visual Science,* 30 (5), 908-918. ISSN: 0146-0404

Jonas, J.B., Thomas, R., George, R., Berenshtein, E. & Muliyil, J. (2003) Optic Disc morphology in south India: the Vellore Eye Study. *British Journal of Ophthalmology,* 87 (2), 189-196. DOI: 10.1136/bjo.87.2.189

Jonas, J.B., Wang Y.X., Zhang, Q., Fan, Y.Y., Xu, Liang, X., Wei, W.B. & Jonas, R.A. (2015) Parapapillary Gamma Zone and Axial Elongation-Associated Optic Disc Rotation: The Beijing Eye Study. *Investigative Ophthalmology & Visual Science,* 57 (2), 396-402. DOI: 10.1167/ivos.15-18263
DOI: 10.1016/j.ophtha.2018.01.026

Kim, M., Kim, T.W., Weinreb, R.N. & Lee, E.J. (2013) Differentiation of Parapapillary Atrophy Using Spectral-Domain Optical Coherence Tomography. *Ophthalmology,* 120 (9), 1790-1797. DOI: 10.1016/j.ophtha.2013.02.011

Kubota, T., Jonas, J.B. & Naumann, G.O.H. (1993) Direct clinic-histological correlation of parapapillary chorioretinal atrophy. *British Journal of Optometry,* 77 (2), 103-106. DOI: 10.1136/bjo.77.2.103

Lee, K.Y.C., Tomidokoro, A., Sakata, R., Konno, S., Mayama, C., Saito, H., Hayashi, K., Iwase, A. & Araie, M. (2010) Cross-sectional Anatomic Configurations of Peripapillary Atrophy Evaluated with Spectral Domain-Optical Coherence Tomography. *Investigative Ophthalmology & Visual Science,* 51 (2), 666-671. DOI: 10.1167/ivos.09-3663

Miki, A., Ikuno, Y., Weinreb, R.N., Asai, T., Usui, S. & Nishida, K. (2019) En Face Optical Coherence Tomography Imaging of Beta and Gamma Parapapillary Atrophy in High Myopia. *Ophthalmology Glaucoma,* 2 (1), 55-62. DOI: 10.1016/j.ogla.2018.11.008

Miki, A., Ikuno, Y., Weinreb, R.N., Yokoyama, J., Asai, T., Usui, S. & Nishida, K. (2017) Measurements of the parapapillary atrophy zones in en face optical coherence tomography images. *PLoS ONE,* 12 (4), e0175347. DOI: 10.1371/journal.pone.0175347

Norwegian electrotechnical publication (2014) Safety of laser products – Part 1: Equipment classification and requirements (NEK IEC 60825-1:2014)

Park, S.C., De Moraes, C.G.V., Tello, C., Liebmann, J.M. & Ritch, R. (2010) In-Vivo Microstructural Anatomy of β-zone Parapapillary Atrophy in Glaucoma. *Investigative Ophthalmology & Visual Science,* 51 (12), 6408-6413. DOI: 10.1167/ivos.09-5100

Ramrattan, R.S., Wolfs, R.C.W., Jonas, J.B., Hofman, A. & de Jong, P.T.V.M. (1999) Determinants of Optic Disc Characteristics in General Population: The Rotterdam Study. *Ophthalmology,* 106 (8), 1588-1596. ISSN: 0161-6420

Reis, A.S.C., Sharpe, G.P., Yang, H., Nicolela, M.T., Burgoyne, C.F. & Chauhan, B.C. (2012) Optic Disc Margin Anatomy in Patients with Glaucoma and Normal Controls with Spectral Domain Optical Coherence tomography. *Ophthalmology,* 119 (4), 738-747. DOI: 10.1016/j.ophtha.2011.09.054

Staurenghi, G., Sadda, S., Chakravarthy, U. & Spaide, R.F. (2014) Proposed Lexicon for Anatomic Landmarks in Normal Posterior Segment Spectral-Domain Optical Coherence Tomography – The IN•OCT Consensus. *Ophthalmology,* 121 (8), 1572-1578. DOI: 10.1016/j.ophtha.2014.02.023

Vianna, J.R., Malik, R., Danthurebandara, V.M., Sharpe, G.P., Belliveau, A.C., Shuba, L.M., Chauhan, B.C. & Nicolela, M.T. (2016) Beta and Gamma Peripapillary Atrophy in Myopic Eyes With and Without Glaucoma. *Investigative Ophthalmology & Visual Science,* 57 (7), 3103-3111. DOI: 10.1167/ivos.16-19646

Wang, Y., Xu, L., Yang, H., Ma. Y. & Jonas, J.B. (2008) Peripapillary atrophy in elderly Chinese in rural and urban Bejing. *Eye,* 22 (2), 261-266. DOI: 10.1038/sj.eye.6702601

Zhang, Q., Wang, Y.X., Wei, W.B., Xu, L. & Jonas, J.B. (2018) Parapapillary Beta Zone and Gamma Zone in a Healthy Population: The Beijing Eye Study 2011. *Investigative Ophthalmology & Visual Science,* 59 (8), 3320-3329. DOI: 10.1167/ivos.18-24141

List of figures, tables and charts

Annexes

Annex 1: Consent form

Annex 2: Protocol for OCT-imaging

Annex 3: Registration form

Annex 4: Frequency of gradual and abrupt ending of IS-OS junction in degree sections

Annex 5: Frequency of overhanging Bruch`s membrane in degree sections

Annex 1: Consent form

Diabetes, syn og øyehelse

Dette er et spørsmål til deg om å delta i ett forskningsprosjekt hvor formålet med prosjektet er undersøke hvordan synsfunksjon, øyehelse og livskvalitet påvirkes hos personer som har type 2 diabetes, og vurdere hvilke undersøkelsesmetoder som er mest effektive for å avdekke syn- og øyeproblemer hos optiker. Resultatene fra prosjektet forventes å gi et vesentlig bidrag til å gjøre optikere i bedre stand til å avdekke syn- og øyeproblemer og håndtere disse målrettet og effektivt, og redusere antallet henvisninger til øyelege.

Du forespørres om å delta fordi du har diabetes type 2 og har blitt invitert gjennom Nasjonalt senter for optikk, syn og øyehelse (NOSØ), Diabetesforbundets lokallag i Buskerud, Telemark og Vestfold, eller gjennom optikere i disse fylkene. Forskningsprosjektet og alle undersøkelser gjennomføres ved NOSØ, Institutt for optometri, radiografi og lysdesign, Fakultet for helse og sosialvitenskap, Høgskolen i Sørøst-Norge, avdeling Kongsberg.

HVA INNEBÆRER PROSJEKTET?

Ved deltakelse i prosjektet vil du bli bedt om å fylle ut spørreskjemaer som avdekker syn- og øyesymptomer og din oppfattelse av livskvalitet knyttet opp mot syn. Du vil gjennomgå undersøkelser som er etter Norges Optikerforbund's retningslinjer. Dette innebærer blant annet: innledende samtale og spørsmål, måling av synsevne, utmåling av eventuelle synsfeil på avstand, samt mikroskopiundersøkelse av fremre og bakre del av øynene. Det vil bli målt øyetrykk, samt at netthinnen din blir avbildet med forskjellige instrumenter. Noen målinger krever at vi drypper med pupilleutvidende dråper. Undersøkelsene som inngår i prosjektet er fordelt over tre besøk, og tidsforbruket vil være ca. 2 timer for hvert besøk. Vi vil også be deg om å komme tilbake til oppfølgende undersøkelse etter 1, 5 og 10 år.

I prosjektet vil vi innhente og registrere opplysninger om deg. Dette er opplysninger som kjønn, alder og resultater fra spørreskjemaer og kliniske tester. Dine opplysninger og resultater vil under prosjektperioden være knyttet til en navneliste gjennom en kode. Kodenøkkelen slettes når datainnsamlingen er avsluttet. Opplysningene som lagres vil i etterkant ikke kunne knyttes til din person.

MULIGE FORDELER OG ULEMPER

Som deltaker i prosjektet får du gjennomført en grundig syn- og øyeundersøkelse. Undersøkelsen inkluderer undersøkelse av tårefilmen, det ytre øyet og netthinnen, og undersøkelser av hvor godt du ser. Det vil bli gitt veiledning og råd som kan gi deg best mulig syn og lindre eventuelle plager for eksempel hvis du har tørre øyne. Dersom det oppdages noen unormale funn, vil vi følge opp dette og sørge for at du får informasjon og eventuell henvisning til øyelege eller lege.

Det er ikke knyttet risiko, betydelig ubehag eller bivirkninger til noen av undersøkelsene. Det vil være nødvendig å bruke øyedråper (Tropikamid 0,5% minims) for å utvide pupillene. Dette kan av noen oppleves litt

ubehagelig da dråpene kan svi noe, og at man blir mer lysømfintlig i etterkant. Effekten av øyedråpene vil avta gradvis og opphører helt etter noen timer. Du bør ikke kjøre bil før synet er normalisert.

Det er gratis å delta i prosjektet.

FRIVILLIG DELTAKELSE OG MULIGHET FOR Å TREKKE SITT SAMTYKKE

Det er frivillig å delta i prosjektet. Dersom du ønsker å delta, undertegner du samtykkeerklæringen på siste side. Du kan når som helst og uten å oppgi noen grunn trekke ditt samtykke. Dette vil ikke få konsekvenser for din videre behandling ved NOSØ. Dersom du trekker deg fra prosjektet, kan du kreve å få slettet innsamlede prøver og opplysninger, med mindre opplysningene allerede er inngått i analyser eller brukt i vitenskapelige publikasjoner. Dersom du senere ønsker å trekke deg eller har spørsmål til prosjektet, kan du kontakte førsteamanuensis Tove Lise Morisbakk (tlf 31 00 97 55, tovelm@usn.no) eller førsteamanuensis Vibeke Sundling (tlf 31 00 89 55, vibeke.sundling@usn.no).

HVA SKJER MED INFORMASJONEN OM DEG?

Informasjonen som registreres om deg skal kun brukes slik som beskrevet i hensikten med studien. Du har rett til innsyn i hvilke opplysninger som er registrert om deg og rett til å få korrigert eventuelle feil i de opplysningene som er registrert.

Alle opplysningene vil bli behandlet uten navn og fødselsnummer eller andre direkte gjenkjennende opplysninger. En kode knytter deg til dine opplysninger gjennom en navneliste.

Prosjektleder, førsteamanuensis Vibeke Sundling, Institutt for optometri, radiografi og lysdesign, Fakultet for helse og sosialvitenskap, Høgskolen i Sørøst-Norge ved Nasjonalt Senter for optikk syn og øyehelse har ansvar for den daglige driften av forskningsprosjektet og at opplysninger om deg blir behandlet på en sikker måte. Informasjon om deg vil bli anonymisert eller slettet senest fem år etter prosjektslutt. Prosjektleder kan kontaktes på tlf: 924 24 360 eller vibeke.sundling@usn.no.

FORSIKRING

Pasientskadeloven.

GODKJENNING

Prosjektet er godkjent av Regional komite for medisinsk og helsefaglig forskningsetikk, (2018/804).

SAMTYKKE TIL DELTAKELSE I PROSJEKTET

JEG ER VILLIG TIL Å DELTA I PROSJEKTET

Sted og dato   Deltakers signatur

Deltakers navn med trykte bokstaver

Jeg bekrefter å ha gitt informasjon om prosjektet

Sted og dato   Signatur

Annex 2: Protocol for OCT-imaging

Protocol: OCT

Instrument: *Cirrus HD-OCT Model 5000 (Zeiss)*

Location: *Room 20*

Preparations

Switch on the instrument and start Acquisition program

- The acquisition program shall start automatically. If not, click the blue icon on the desktop: "Cirrus HD-OCT"
- Username: *Cirrus Operator*
- Password: (no password)

Prepare for use

- Remove lens cap and check clearness of the lens.
  If necessary, use dedicated lens paper and solution to remove stain by gentle rotational movement along a spiral path from centre to periphery of the lens.
- Click "Add New Patient" and enter patient information, or click "Find Existing Patient"

Choose sequence of eyes

- Right followed by left or Left followed by right selected from log
- Register and cross out in log
- Acquisition will be in the same sequence for both eyes:
  - Macula: **(1) Macular Cube (200x200), (2) HD 1 line 100x (with "EDI"), (3) HD Raster 5 (with "EDI")**
  - Optic Disc: **(4) Optic Disc Cube (200x200), (5) HD Radial**

Preparation for imaging

- Clean chin- and headrest with alcohol
- Reduce illumination in room
- Position subject and align head
- Give instructions
- Select patient and click "Acquire" (bottom right on the screen)

1

Acquisition - Macula:

SELECT THE FOLLOWING SCAN MODES FOR MACULAR SCANS:

1) **Macular Cube 200x200**
2) **HD 1 Line 100x**
3) **HD Raster (1 or 5 lines)**

1. Find the pupil and focus the image in the iris viewport.

Adjust table height.

Place patient's chin in the left chin cup (marked blue) to scan the right eye or the right chin cup (marked white) to scan the left eye. Patient's forehead should make contact with the headrest. Adjust the chinrest height to align the canthus marker with the patient's eye

Adjust the patient position to find the iris and pupil. Use the chinrest controls or click on the pupil in the iris viewport. Instruct the patient to move with the chinrest. The patient should not hold on to instrument. Click within the center of the pupil for final alignment.

Use [ ] to obtain a clear focus on the iris. This helps the system set the position for the OCT scan.

Advanced Tips

- Click on the [ ] icon to adjust the brightness, contrast, and illumination. Lowering the illumination may increase pupil size.
- The mouse scroll wheel can be used to make fine changes to the iris image in/out adjustment.
- During subsequent steps, monitor: 1) the patient's head to ensure they maintain contact with the headrest and, 2) the position of the red scan circle in the pupil to ensure it remains within the pupil.

2. Make adjustments for optimal fundus and B-scan images.

Click on **Auto Focus**. Instruct patient to move with the chinrest, fixate on the target and to not blink while this function runs. Adjust manually if necessary. Proper focus can increase the signal for the OCT scans and improve ability to track.

Click on **Optimize** to center and enhance the B-scan images. To sharpen the fundus image, mouse over the fundus image and click on the wand that appears in the upper right corner to perform auto B/C.
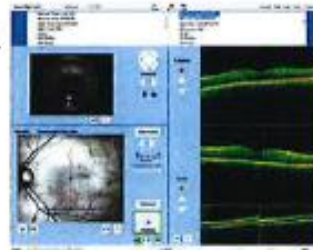

Performing a scan with FastTrac™

- When the border around the **Capture** button is green, you are ready to acquire the scan with FastTrac. If the border is red, further actions can be taken:
- Center the scan with the **Center** controls or hold **Shift** and roll the mouse wheel.
- Click **Auto Focus** or manually adjust focus to sharpen fundus image quality.
- Change the prior scan or disable **Track to Prior** button [ ] for this scan.
- You can turn off tracking by clicking the FastTrac button [ ].

Advanced Tips

- The B-scan images should show a range of colors. Faint green B-scans indicate that the signal is low.
- To modify brightness or contrast for either the B-scans or fundus images, click [ ] near the image of interest and adjust the controls. Note: The setting changes made for the B-scans here will persist for future scans.
- If the OCT image appears inverted, click the **Center** up/down buttons several times until the image flips and is centered it in the window.
- Center the B-scan images and ensure all B-scan images are not too high or too low. This could result in missing data in the scan.
- For highly myopic patients it may be necessary to click the **Auto Focus** button a second time.
- Moving the scan in the pupil in the iris viewport can help if: 1) there are media opacities, 2) the OCT B-scans appear tilted.
- Instead of using **Auto Focus**, enter spherical equivalent information on the patient demographic page for CIRRUS to pre-focus to this value.
- When tracking on the macula with patients with tilted retinas, you can improve success using tracking by turning off the system's center position monitoring. Click on the wand next to the bottom B-scan, then in the dialog box, uncheck **Monitor Z position**.

2

Note: For scan 2) and 3), select the "EDI" checkbox (= Enhanced Depth Imaging)
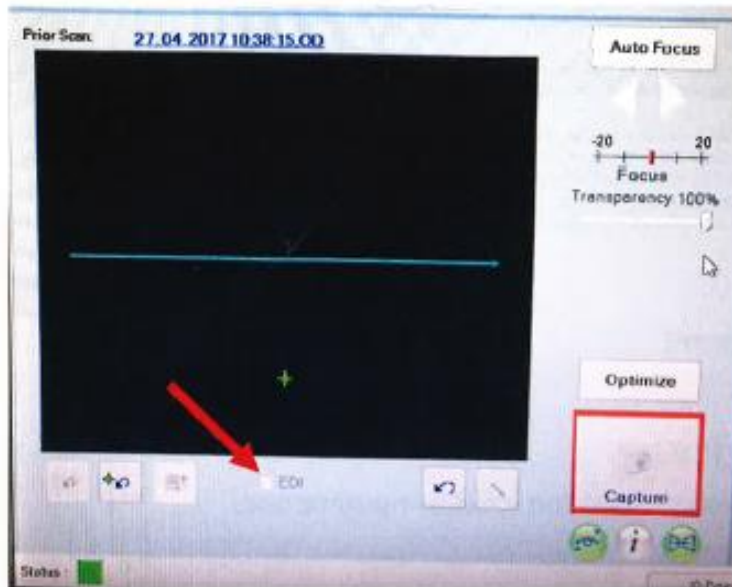
3. Capture the fundus image and high-density scan.

When the fundus image and B-scans are optimized, tell the patient to blink once or twice. Then tell the patient to open wide and maintain focus on the center of the green fixation target.

Click **Capture**

Avoid a patient blink right at the moment you intend to click **Capture**

If tracking is on, you can tell the patient to blink naturally during the scan.

If tracking is off, remind the patient to avoid blinking and to focus on the target until the capture is completed.

> **FastTrac Scan In Progress Screen.** When FastTrac is interrupted, the progress bars turn red and processing stops. Click **Cancel** to return to the Acquire Screen to make adjustments to center the scan, focus the fundus or iris images, or turn off FastTrac for a non-tracked scan.
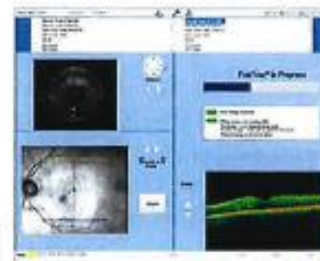
### 4. Review the captured scan, then save or try again.

On the Review screen, evaluate the B-scan quality and the Signal Strength (6 or greater). Check that the OCT B-scans are approximately centered in the windows without missing data.

If scan quality, position, or eye movements are unacceptable, click **Try Again** to retake the scan.

Adjust brightness and contrast by right clicking on the fundus or OCT image. The B/C values set on the review screen are saved and used for analysis for this scan only.

Click **Save**

If you perform another scan on the same eye, the patient can stay positioned. Otherwise, the patient should sit back.

3
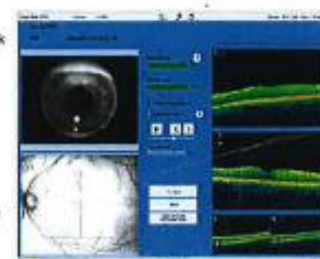
Advanced Tips

- Examine the high definition en face scan closely for any subtle eye movement. Also slide the **Transparency** control back and forth to compare the images.
  If noteworthy movement is detected, click **Try Again**.
- If the next scan will be on the other eye, choose the scan pattern for that eye before the patient returns their head to the appropriate chin cup and headrest. This can help avoid contact with the patient's nose.
- During a scan with FastTrac, individual B-scans in a cube may be acquired at slightly different positions, resulting in horizontal lines or bands on the fundus image. If there are no saccades, a scan with bands in the OCT fundus should be acceptable for analysis.
- Smart HD Scans automatically find the fovea based on the Macular Cube scan information. You can also use the Macular Cube to target a specific feature for a Smart HD Scan.

Example: Saccades
(vessel mismatch)

Example: Banding
(no vessel mismatch)

Repeat protocol for the other eye.

Acquisition - Optic Disc:

SELECT THE FOLLOWING SCAN MODES FOR SCANS OF THE OPTIC DISC:

4) **Optic Disc Cube 200x200**
5) **HD Radial**

Follow the same instructions as for macular scans. The fixation target for scan number 4) will be automatically moved to one side. Instruct the subject to fixate at the green target before you capture the images.

For scan number 5), make sure that the optic disc is in the centre of the fundus image. If not, move the fixation target by moving the green cross to the side as shown below (red arrows). Make sure that the optic disc is in focus and centred before capturing the images. The white lines, which are the scan patterns, has to be in the centre of the optic disc. Move the scan pattern with by dragging the pattern with the mouse, and position it centrally.
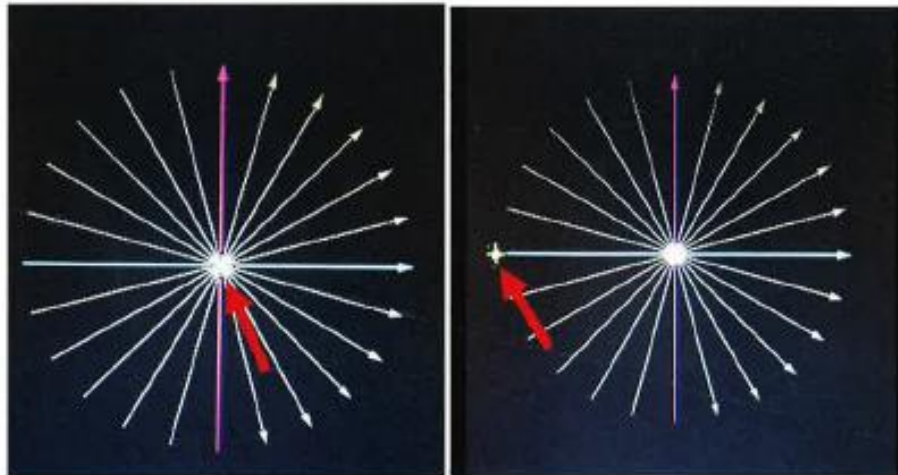
Repeat protocol for the other eye.

QUALITY CHECK

Make sure that all five scans for both eyes have sufficient quality. Before saving each scan, make sure that the "quality bars" are green.

1 Iris image
2 Fundus image with scan cube overlay with blue and magenta slice navigators
3 Current X slice through front (fast B-scan)

4 Current Y slice through side (slow B-scan)
5 X slices through front and back (fast B-scans)
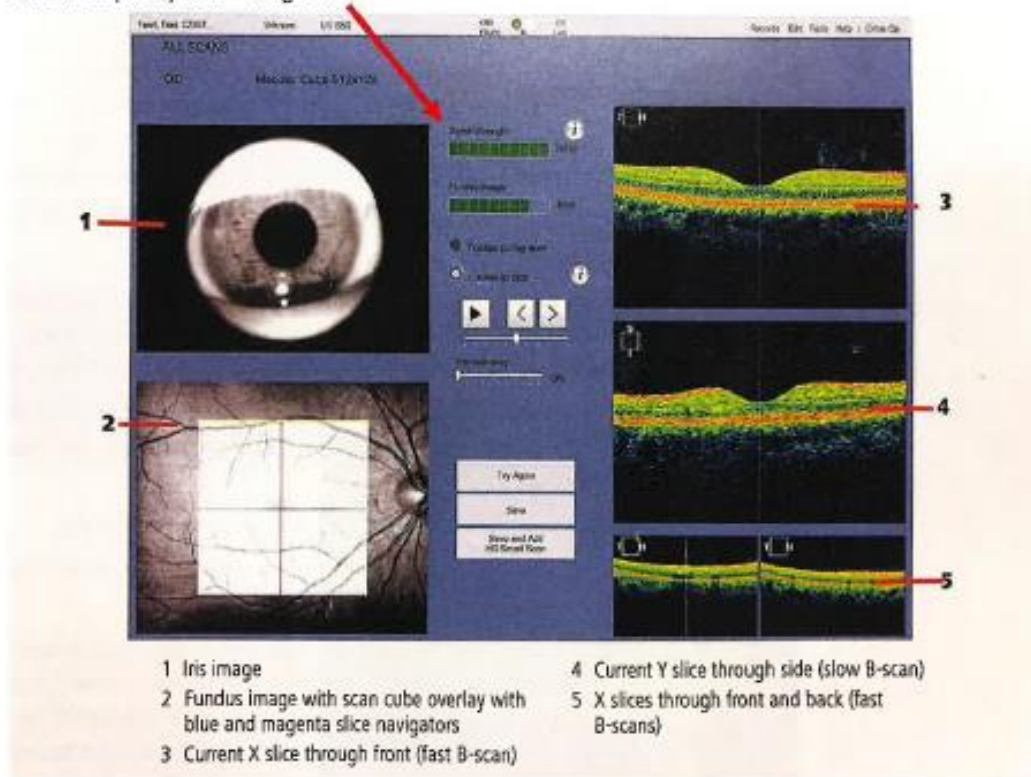
Check the image quality on the screen. If the quality is considered to be insufficient, a new OCT-scan is taken until satisfactory quality has been obtained.

Criteria for Image Acceptance:
Fundus

- Make sure that the focus is sharp and clear, good visibility of vessels.
- Scan overlay should be centered on the fovea or optic disc.
- Fundus image should have uniform illumination without dark corners
- There should be no artifacts (or few) that may cast shadow on the OCT scan.
- The OCT *En Face* image should have minimal saccades and no saccades through the area of interest
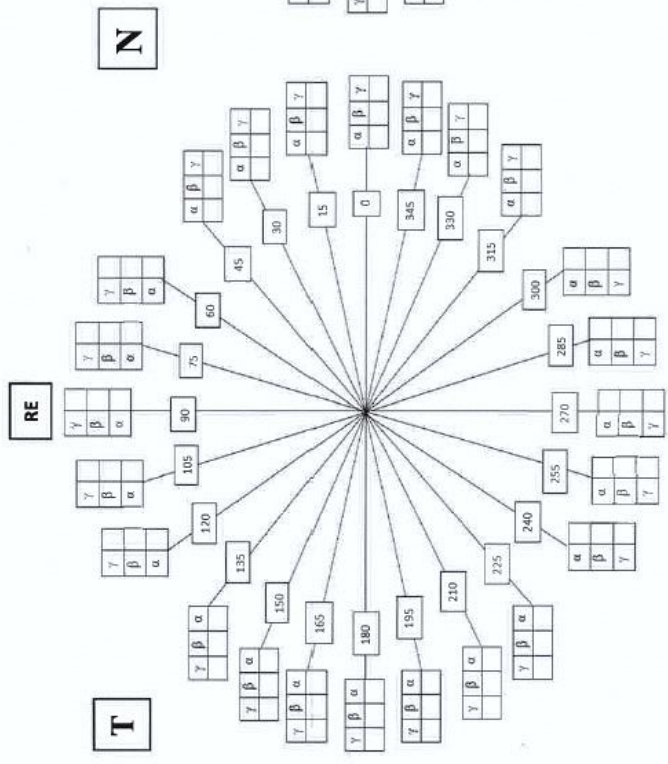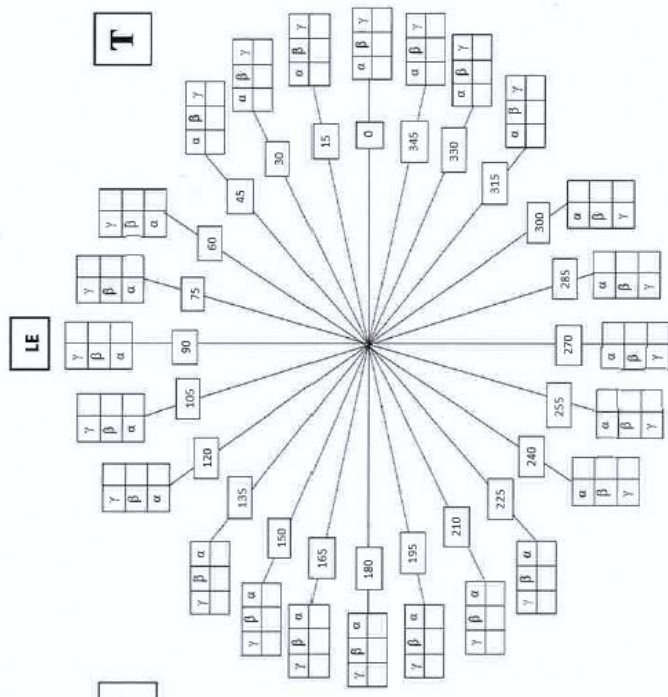
OCT

- OCT scan must be complete in all windows without missing data
- Color density should be the same from end to end.
- Signal strength should be 6 or higher (> 5/10)

5

Annex 3: Registration form

Parapapillary atrophy registration form

Annex 4: Frequency of gradual and abrupt ending of IS-OS junction in degree sections

Degrees	RIGHT EYES			LEFT EYES		
	Eyes w/ alpha N	Gradual ending n (%)	Abrupt ending n (%)	Eyes w/ alpha N	Gradual ending n (%)	Abrupt ending n (%)
0	58	55 (94.8)	3 (5.2)	56	48 (85.7)	8 (14.3)
15	58	56 (96.6)	2 (3.4)	55	51 (92.7)	4 (7.3)
30	52	48 (92.3)	4 (7.7)	50	46 (92.0)	4 (8.0)
45	51	49 (96.1)	2 (3.9)	50	48 (96.0)	2 (4.0)
60	45	45 (100)	0 (0)	43	42 (97.9)	1 (2.3)
75	45	42 (93.3)	3 (6.7)	45	45 (100)	0 (0)
90	34	31 (91.2)	3 (8.8)	39	39 (100)	0 (0)
105	40	38 (95.0)	2 (5.0)	44	43 (97.7)	1 (2.3)
120	45	45 (100)	0 (0)	44	43 (97.7)	1 (2.3)
135	40	40 (100)	0 (0)	47	47 (100)	0 (0)
150	49	47 (95.9)	2 (4.1)	48	47 (97.9)	1 (2.1)
165	55	54 (98.2)	1 (1.8)	47	44 (93.6)	3 (6.4)
180	56	55 (98.2)	1 (1.8)	49	45 (91.8)	4 (8.2)
195	57	56 (98.2)	1 (1.8)	47	46 (97.9)	1 (2.1)
210	52	48 (92.3)	4 (7.7)	48	48 (100)	0 (0)
225	46	45 (100)	0 (0)	36	34 (94.4)	2 (5.6)
240	39	37 (94.9)	2 (5.1)	35	35 (100)	0 (0)
255	45	45 (100)	0 (0)	42	42 (100)	0 (0)
270	36	36 (100)	0 (0)	40	38 (95.0)	2 (5.0)
285	41	41 (100)	0 (0)	48	48 (100)	0 (0)
300	42	41 (97.6)	1 (2.4)	46	44 (95.7)	2 (4.3)
315	50	49 (98.0)	1 (2.0)	51	49 (96.1)	2 (3.9)
330	53	51 (96.2)	2 (3.8)	52	47 (90.4)	5 (9.6)
345	58	53 (91.4)	5 (8.6)	52	50 (96.2)	2 (3.8)

Annex 5: Frequency of overhanging Bruch`s membrane in degree sections

Degree	RIGHT EYES			LEFT EYES		
	Eyes wo/ beta N	No overhang n (%)	Overhang n (%)	Eyes wo/ beta N	No overhang n (%)	Overhang n (%)
0	20	18 (90.0)	2 (10.0)	21	21 (100)	0 (0)
15	24	21 (87.5)	3 (12.5)	18	15 (83.3)	3 (16.7)
30	23	22 (95.7)	1 (4.3)	19	17 (89.5)	2 (10.5)
45	23	18 (78.3)	5 (21.7)	22	20 (90.9)	2 (9.1)
60	22	16 (72.7)	6 (27.3)	20	16 (80.0)	4 (20.0)
75	24	19 (79.2)	5 (20.8)	19	12 (63.2)	7 (36.8)
90	20	16 (80.0)	4 (20.0)	14	10 (71.4)	4 (28.6)
105	25	20 (80.0)	5 (20.0)	19	11 (57.9)	8 (42.1)
120	27	24 (88.9)	3 (11.1)	17	9 (52.9)	8 (47.1)
135	21	16 (76.2)	5 (23.8)	17	8 (47.1)	9 (52.9)
150	32	21 (65.6)	11 (34.4)	25	18 (72.0)	7 (28.0)
165	43	30 (69.8)	13 (30.2)	32	26 (81.3)	6 (18.8)
180	44	30 (68.2)	14 (31.8)	39	29 (74.4)	10 (25.6)
195	45	32 (71.1)	13 (28.9)	36	24 (66.7)	12 (33.3)
210	39	30 (76.9)	9 (23.1)	32	25 (78.1)	7 (21.9)
225	31	29 (93.5)	2 (6.5)	24	18 (75.0)	6 (25.0)
240	25	20 (80.0)	5 (20.0)	21	15 (71.4)	6 (28.6)
255	25	20 (80.0)	5 (20.0)	27	22 (81.5)	5 (18.5)
270	19	16 (84.2)	3 (15.8)	19	15 (78.9)	4 (21.1)
285	24	23 (95.8)	1 (4.2)	25	20 (80.0)	5 (20.0)
300	20	18 (90.0)	2 (10.0)	22	20 (90.9)	2 (9.1)
315	19	18 (94.7)	1 (5.3)	27	24 (88.9)	3 (11.1)
330	18	17 (94.4)	1 (5.6)	24	22 (91.7)	2 (8.3)
345	17	15 (88.2)	2 (11.8)	19	17 (89.5)	2 (10.5)